Heliyon 10 (2024) e32495

Contents lists available at ScienceDirect

Heliyon

journal homepage: www.cell.com/heliyon

Review article

Weibull analysis of ceramics and related materials: A review

Obinna Anayo Osuchukwu [a,i,*], Abdu Salihi [a], Abdullahi Ibrahim [a], Adamu Abdullahi Audu [a], Mahdi Makoyo [a], Sikiru Adepoju Mohammed [c], Mohammed Y. Lawal [c], Precious Osayamen Etinosa [d], Ibitoye Opeyemi Isaac [e], Peter Gbenga Oni [f], Oreoluwa Gabriel Oginni [g], David Olubiyi Obada [b,h,i,**]

[a] *Department of Mechanical Engineering, Bayero University, Kano, 700241, Nigeria*
[b] *Department of Mechanical Engineering, Ahmadu Bello University, Zaria, 810222, Nigeria*
[c] *Mechanical Engineering Department, Nigerian Defence Academy, Kaduna, PMB 2109, Nigeria*
[d] *Department of Mechanical Engineering, Worcester Polytechnic Institute, 100 Institute Road, Worcester, MA 01609, USA*
[e] *Department of Biology and Biotechnology, Worcester Polytechnic Institute, 100 Institute Road, Worcester, MA 01609, USA*
[f] *Department of Chemistry and Biochemistry, Worcester Polytechnic Institute, 100 Institute Road, Worcester, MA 01609, USA*
[g] *Brown School, Washington University 1 Brookings Dr, St. Louis, MO 63130, USA*
[h] *Africa Centre of Excellence on New Pedagogies in Engineering Education, Ahmadu Bello University, Zaria, 810222, Nigeria*
[i] *Multifunctional Materials Laboratory, Shell Office Complex, Department of Mechanical Engineering, Ahmadu Bello University, Zaria, 810222, Nigeria*

ARTICLE INFO

Keywords:
Ceramics
Hydroxyapatite
Orthopaedic implants
Reliability
Weibull modulus

ABSTRACT

It has been realized throughout the years that an ideal combination of high toughness, hardness and strength is required in many engineering applications that need load-bearing capabilities. Ceramics and related materials have significant constraints for structural and particular non-structural applications due to their low toughness and limited strength while having substantially superior hardness than typical metallic materials. For example, hydroxyapatite (HAp) has gained attention for applications in orthopaedic implants, dental materials, drug delivery, etc. Researchers have continued to strive to produce HAp materials with reliable properties within the acceptable Weibull modulus (*m)* for load bearing. The Weibull analysis (WA) is a statistical analysis adopted widely in reliability applications to detect failure periods. Researchers have confirmed it to be an effective technique to get results on the reliability of materials at a moderately low rate with assured reliability of the material or component. This review summarizes the WA and the steps in the Weibull method for its reliability analysis to predict the failure rate of ceramics like HAp and other related materials. Also, the applications of WA for these materials were reviewed. From the review, it was discovered that Weibull distribution is proven to confer to the feeblest-link concept. For brittle materials, it was revealed that the Weibull Modulus ranges from 2 to 40, and environment, production processes, and comparative factors are well-thought-out contributing factors for reliability. In addition, the confidence interval can be up to 95 %. The frequently used technique for reliability valuation is to syndicate the Weibull statistics. Also, a very narrow distribution is desirable to offer the expected likelihood. Furthermore, when paired with trials, Monte Carlo simulations prove to be a very helpful tool for forecasting the dependability of different estimate techniques and their optimization. Finally, if

* Corresponding author. Department of Mechanical Engineering, Bayero University, Kano, 700241, Nigeria.
** Corresponding author. Department of Mechanical Engineering, Ahmadu Bello University, Zaria, 810222, Nigeria.
E-mail addresses: oao1800004.pme@buk.edu.ng (O.A. Osuchukwu), doobada@abu.edu.ng (D.O. Obada).

https://doi.org/10.1016/j.heliyon.2024.e32495
Received 30 September 2023; Received in revised form 3 June 2024; Accepted 5 June 2024
Available online 6 June 2024

the equivalent m is anticipated to be high, it signifies that the material has a high degree of homogeneity of properties and high reliability. WA can find application in predicting the dependability and lifetime of materials, making it widely utilized in engineering and other disciplines. It is especially useful for analysing data in which the likelihood of failure per unit of time varies over time.

1. Introduction

The restoration of bone defects and osteoporosis are two significant challenges in bone repair activities that require the reliability of the implant material [1–3]. Several techniques, including plasma spraying, and hydroxyapatite (HAp) coatings are used to achieve osseointegration and graft external treatment [4–7]. However, HAp and other porous coating materials are the most often used remedies today [8]. Using a coating layer aims to achieve effective osseointegration and critical bone-implant interaction. Researchers have continued to investigate the production of HAp scaffolds for bone tissue applications in recent years because of their essential bioactivity and osteoconductivity [9]. HAp is an inorganic bio-ceramic component of natural bones and teeth with high biocompatibility, osteoinductivity, surface area (100 $m^2\ g^{-1}$), and bioactivity [10–12]. HAp has the following characteristics: The apatite molecular formula is $Ca_5(PO_4)_6(OH)_2$, similar to human apatite, which has a Calcium - Phosphate ratio of 1.67.

HAp has been confirmed by different researchers to be the most stable biomaterial with these basic qualities (biocompatibility, osteoinductivity, and bioactivity) when employed in bone repair [13]. The bones of cattle or bovine, camels, horses, and fish can produce natural HAp. Egg shells, plants, algae, and limestone can also produce it [14–22]. In the work conducted by [23], some of the physiochemical, mechanical, and biological characteristics of HAp, and some of the methods for producing HAp powder were listed. The composite biomaterials like synthetic or natural polymers plus HAp have mechanical properties most similar to human bone tissue [24]. HAp has low fracture toughness and flexural strength, which prevents it from being used as a graft material on a large scale in orthopaedics and dentistry [25]. As a result, in the field of biomedical engineering for bone implants, their mechanical qualities and reliability are critical. One way to determine the reliability of ceramic materials is through Weibull statistical analysis by knowing the Weibull modulus, m [26–29]. Numerous methods have been employed to measure the Weibull modulus, m, and its physical consequences on the statistical distribution of fracture strengths in brittle materials [30]. Despite the importance of the Weibull modulus, m, as a measure of the mechanical reliability of ceramic materials, only a few research reports are available on the Weibull modulus and fracture strength of HAp. Weibull Analysis (WA) is a statistical approach for analyzing a material's life cycle statistics. The results of measuring a product's life are known as life statistics [31]. Failure analysis is a dynamic system of understanding a system's consistent features and activities, employing a minimal model scope of the area [32–37]. WA is a valuable tool for determining a product's lifetime performance. Weibull techniques can be used to evaluate sample data acquired concerning failures and time to aid in responding to major concerns [38]. The capacity to investigate failure tendencies and provide failure predictions based on known sample data sets is the main value of WA, which is related to its flexibility and ability to apply to small sample sets quickly. It also provides a visual and graphical representation of failure data [39–41].

A technique for assessing life data is WA. Measurements of a product's life yield its life data. Product life data is measured in hours, miles, number of cycles, or other metrics that are used to determine a product's efficient functioning, depending on the product or industry [42]. Weibull analysis's main benefits are as follows: It may provide fairly precise failure assessment and failure predictions with tiny data samples, enabling solutions to be implemented as soon as a flaw is detected [43–46,47]. The Weibull distribution is extensively employed in failure time prediction due to the large range of probability curve shapes that may be produced by varying the two parameters, β (shape parameter), and α (scaling parameter) [48,49]. Even though the procedure of the normal distribution normally involves at least 20 failures or facts from previous experience, WA works exceedingly fine when there are as limited as 2 or 3 failures, which is serious when the result of a failure comprises safety costs. Other advantages of Weibull distribution include [50–52]:

(i) It is expansively used to assess mechanical, chemical, and material failures.
(ii) Afford discreetly precise failure analysis and failure predictions with very small data samples, making results likely at the earliest signs of a problem.
(iii) Afford modest and valuable graphical plots for distinct failure modes that can be simply read and understood, even when data insufficiencies occur.
(iv) Signify a wide array of distribution shapes so that the distribution with the finest fit can be selected.
(v) Afford physics-of-catastrophe signs according to the slope of the Weibull possibility.

Some research has been done to buttress these advantages. To evaluate the mechanical reliability of porous HAp, Pires et al. [53] employed WA to investigate the fracture toughness of dense polycrystalline HAp bioceramic made from cow bones after adding ZnO/TiO_2 nanoparticles and TiO_2 nanotubes. The WA results indicated that adding 5 % of TiO_2 nanoparticles improved the Weibull parameter (m), but there was no statistically significant variation from the pure HAp. ZnO_2 nanomaterials at a 5% proportion reduced the HAp characteristic strength without altering m. Fan et al. [54] studied the strength of extremely porous HAp. The partly sintered HAp samples were cracked in biaxial flexure using a ring-on-ring examination fitting. The fracture strength declined monotonically with declining sintering temperature from 4.8 MPa for samples sintered at 1025°C–0.66 MPa for samples sintered at 350°C. However, the value of m rose unexpectedly, extending from 6.6 to 15.5. Ćurković et al. [55] employed WA to investigate the flexural strength of alumina ceramics. The three-point bend test was used to determine the flexural strength of standard purity alumina ceramics. Flexural strength was determined to be between 266.7 and 357.5 MPa. The numerical randomness of flexural strength calculated by the three-point bend test was investigated using a two-parameter Weibull distribution (W_d) function. Flexural strength was measured at 17.4 Wm. They concluded that this restriction can be used to characterize the variability in the tested material's flexural strength as well as its consistency. What matters most for the mechanical characteristics of brittle materials (bioceramics) is the Weibull modulus, *m* [56]. In the production of bioceramics, the *m* can also be influenced by the following factors in addition to the microstructure: powder treating methods [57], strength evaluation methods [58], rate of loading [59,60], particle size and form [61], and finishes on the surface [62,63]. A two-parameter WA can be employed to evaluate the fracture data of valid cracked samples [64,65]. Generally speaking, only moderately dense bioceramic samples are covered in the literature when discussing the *m* of brittle materials [66].

Bioceramics belong to a family of biomaterials employed in biomedical engineering. Because of their versatility in fabrication, high compressive strength, variable porosity, and bioactive qualities in the body, ceramics are frequently employed as implant materials [67]. This type of biomaterial can be synthesized from bovine and catfish bones [68–72]. The boom in bovine and catfish farming in Nigeria has led to a substantial upsurge in the creation of bone biowastes. These biowastes can be used as raw material for producing HAp, a pervasive calcium phosphate substance used in biomedical engineering [73]. The economy, environment and general health could all significantly gain from this conversion of biowastes [74]. The conversion of these biowastes into HAp is a good development, but the analysis to determine or predict its reliability using WA is of great importance and is challenging. This review summarizes the overview of WA and some steps in the Weibull method for its reliability analysis to predict the failure rate of HAp. Also, the applications of HAp are presented. This review thus serves as a reference for further advanced studies on determining the *m* of naturally derived HAp from an array of sources like bovine and catfish bones to predict its reliability.

2. Overview of Weibull analysis (WA)

Weibull distribution is proven to confer to the feeblest-link concept [75–78]. For brittle materials, the literature revealed that environs, production processes, and comparative factors are well-thought-out contributing factors for reliability [79–82]. The frequently used technique for reliability valuation is to syndicate the Weibull statistics [83]. In this condition, the strength is defined as a definite distribution but not a single numeral. The estimated *m* from strength distribution can reveal the strength potential of the material investigated. A very narrow distribution is desirable to offer likelihood. The equivalent *m* is anticipated to be high, signifying the material has a high degree of homogeneity of properties and high reliability [84–87]. For materials with a homogeneous flaw density, Weibull analyzes fracture statistics [39].

WA is a widely utilized distribution in the analysis of reliability and durability data. The Weibull distribution may describe diminishing, cumulative, or constant risk functions, allowing it to define any stage of the item's life cycle [88–93]. Waloddi Weibull introduced a statistical distribution in 1939 that frequently defines identified failures. Weibull's distribution was given as a single specialized subject. The distribution was based on Pierce's concept of the "weakest link," and since then, it's been broadly used to evaluate the fracture-related mechanical properties of ceramics and metals. Equation (1) below gives the cumulative probability function of Weibull two parameters, Wd [94–97]:

$$P = 1 - exp\left[-\left(\frac{x}{xo}\right)^{m}\right] \tag{1}$$

where P = probability of failure at a given fatigue life, x, or lower; x_o and *m* are scale and shape parameters, respectively.

The following assumptions support the Weibull model [98]:

1. The sum of defects alleged in one intermission is autonomous for a fixed group of time. The number of detected failures is indiscriminate at this point.
2. At the start of the period in which the package is noticed, there is a fixed number of flaws (N) in the package. In life testing, taking the logarithms of the failure times is usual. The log failure times have a normal distribution if the log-normal distribution is the assumed distribution. The assumption that the lifespan follows a Weibull distribution is more widely held. In this instance, the distribution of the log failure times is location-scale rather than typical.
3. The period of defects of failure is scattered as a Weibull distribution with parameters x_o and m. In Weibull regression, it is typically assumed that the shape parameter is constant and the scale parameter depends on the predictor variables.
4. A defect is amended instantly deprived of presenting new defects in the package. When choosing an experimental design, one should take the number of parameters that need to be estimated into consideration. All of the model's parameters should be estimable by the design.

We can formally simulate the interaction if assuming a common shape parameter, x_o, for the Weibull distribution (or constant scale parameter *m* in the distribution). For instance, Dey et al. [99] disclosed that the individual data of nano-hardness and Young's modulus were estimated with the aid of Weibull statistics. As the indentation stress was increased from 10 to 1000 mN, the Weibull moduli data for both the nano-hardness and Young's modulus of the MIPS-HAp coating increased. The W_d fixtures for the nano-hardness value of the coating are presented for the low (10–100 mN) loads and the high (300–1000 mN) loads. Recently, Tiryakioglu and Campbell [100,101] presented procedures for understanding Weibull probability plots as well as the three-parameter Weibull distribution and Weibull combinations. Their result showed that ceramics, with their low-fracture toughness, are also likely to yield fracture properties that will trail the two-parameter Weibull distribution. According to Ref. [102], the Weibull distribution (W_d) is elastic to diverse distributions.

In conclusion, the use of W_d has three great advantages [103]:

1. It can precisely model quality and performance characteristics (PC), and its elasticity brands it supreme for use in analyzing a dataset with an unknown distribution.
2. Following that, it denotes a significant quantity of a task.
3. It gives precise failure investigation and hazard forecasts with trivial models.

The parameters have actual denotation and *m* shows whether the rate of the measured PC is increasing, steady, or falling at its current rate. A $\beta < 1.0$ shows that the feature is decreasing, while an $\alpha > 1.0$ shows that it is an upward rate (Fig. 1).

2.1. Graphical representation of Weibull parameters

The shape, β, parameter depicts the distribution's shifts from 0, with a negative shape indicating a shift to the left of 0 and a positive shape indicating a shift to the right. The scale parameter, α, is the statistics' 63.2 percentile, and it represents the Weibull arc's link to the shape in the same way as the mean characterizes the place on a standard curve. The Weibull curve's shape is determined by the shape parameter. The properties of distinct dissimilar life dispersals can be perfected by modifying the shape [109,110]. The 63.2 percentile of the distribution is the Weibull scale parameter (α) [111]. This indicates that, for instance, 63.2 % of the observed values will be less than 2 if a Weibull distribution with $\alpha = 2$ is used. The image that follows illustrates how the scale parameter changes while maintaining a constant shape parameter ($\beta = k = 3.5$) (Fig. 2).

As illustrated by Liu et al. [112] (Fig. 3a), the scale parameter for 80 % of the 205,873 fitted Weibull Probability Density Function (PDF) was less than 70 s. This indicates that 63.2 % of all observations for those 80 % of probabilities had a dwell time value of less than 70 s. The distribution's plan is modelled by the shape parameter, β. An exponential distribution replaces the Weibull distribution if $\beta = 1$. A normal distribution is comparable to the Weibull probability density function (PDF) when β is between 3 and 4. Consider Fig. 3b which represents a Weibull PDF with a steady shape parameter ($\beta = 20$) varied from 0.5 to 2, 3.5, and 8 [112].

2.1.1. Weibull Distribution with shape < 1

When β is between 0 and 1, the graph displays that the likelihood declines exponentially from infinity. About the catastrophe rate, the value that this distribution has is a greater number of early failures, which declines over the period as the faulty samples are removed from the model. Since these failures occur in the early period of an item's life, it is referred to as "infant mortality" [113–117]. In this review hereafter, the scale parameter, α is replaced with x_o, the shape parameter, β is replaced with m, and the threshold parameter, γ is replaced with y_o. Fig. 4a shows a typical Weibull distribution with the shape parameter less than 1.

2.1.2. Weibull Distribution with shape = 1

If *m* is equal to 1, the W_d declines exponentially from $1/x_o$, where x_o = the scale parameter. This proves that with time, the failure degree is steady. This shape is suitable for haphazard catastrophes and multiple-cause catastrophes, which can be adapted to perfect the valuable life of items [118]. Fig. 4b shows a typical Weibull distribution with the shape parameter equal to 1.

2.1.3. Weibull Distribution with Shape between 1 & 2

When *m*, is between 1 and 2, the Weibull Distribution increases to its highest rapidly, before declining over time. The failure rate

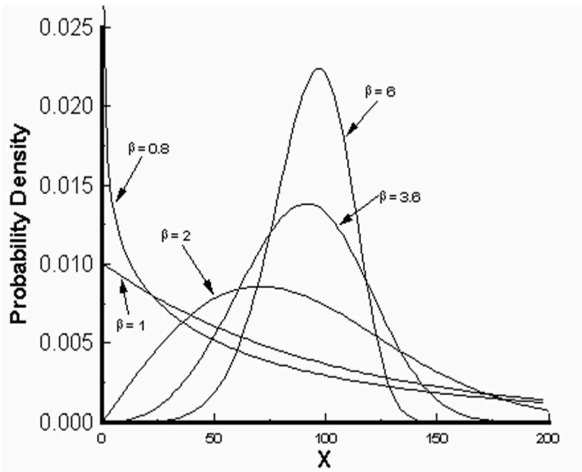

Fig. 1. Typical of Weibull distribution showing the shape parameters [104–108].

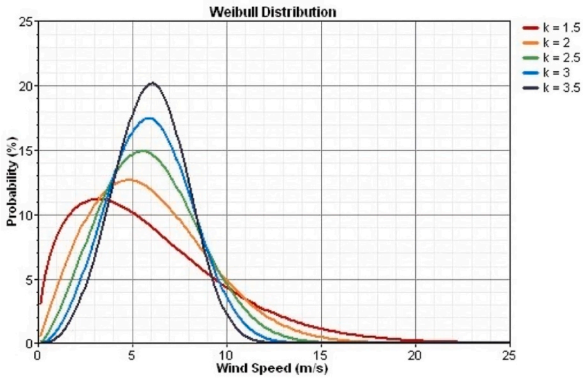

Fig. 2. Typical Weibull distribution plot [111].

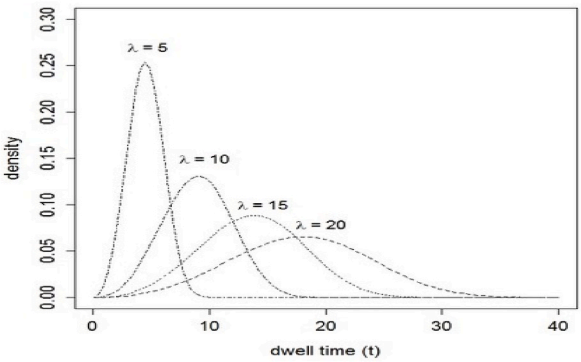

Fig. 3a. Typical 63.2 % Weibull distribution showing shape parameters [112].

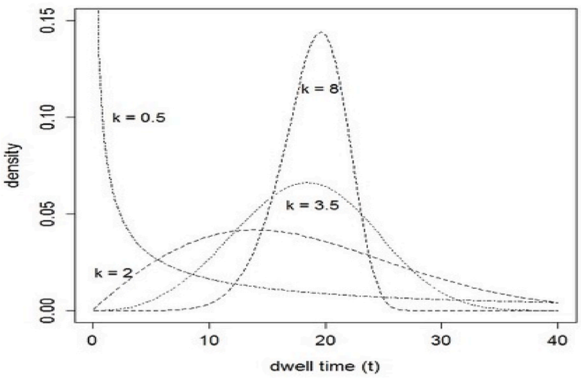

Fig. 3b. Typical 63.2 % Weibull distribution with varied shape parameters [112].

rises completely, with the quickest rise happening first. This shape is revealing premature failures due to wear and tear [116,119]. Fig. 4c shows a typical Weibull distribution with the shape parameter between 1 and 2.

2.1.4. *Weibull Distribution with shape = 2*

The direct growing failure rate is when m = 2, in which the risk of wear-out failure climbs progressively during the item's lifetime. The Rayleigh distribution describes the Wd's characteristics [120–122]. Fig. 4d shows a typical Weibull distribution with the shape parameter equal to 2.

2.1.5. *Weibull Distribution with Shape between 3 & 4*

If *m* is between 3 and 4, the Wd is symmetrical and bell-shaped, just like the typical curve. This Wd approach simulates quick wear-

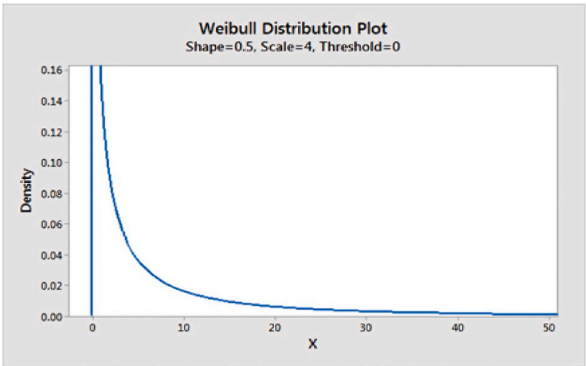

Fig. 4a. Typical Weibull distribution with shape parameter less than 1 [116].

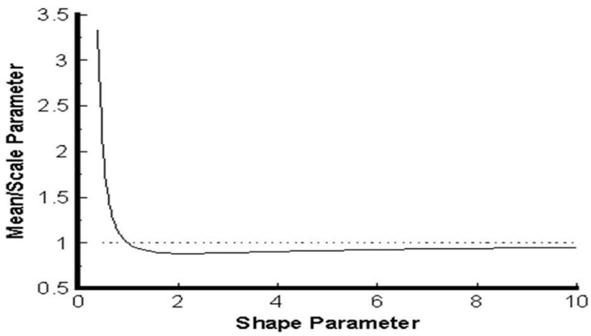

Fig. 4b. Typical Weibull distribution with shape parameter equal to 1 [116,118].

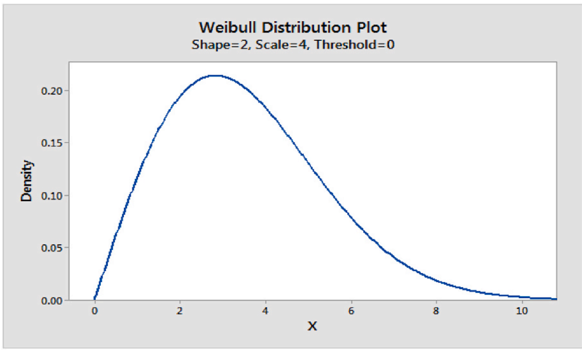

Fig. 4c. Typical Weibull distribution with shape parameters between 1 and 2 [116].

out failures in the final stages of an item's life when maximum disasters occur [120]. Fig. 4e shows a typical Weibull distribution with the shape parameter between 3 and 4.

2.1.6. Weibull Distribution with shape > 10

When m > 10, the Wd resembles an end data distribution, and this distribution system can perfect the ultimate passé of a product lifespan [117,123,124]. Fig. 4f shows a typical Weibull distribution with the shape parameter greater than 10.

Considering the bathtub graph shown in Fig. 5, a typical failure pattern and several stages can be noticed. One specific kind of failure rate graph is the bathtub curve. The deterioration prediction and reliability engineering both make use of this graph. The term 'bathtub' describes a line with two edges of the curve that resemble a bathtub. Three areas make up the bathtub curve [125,126]:

(i) Because of these early failures, the first region has a declining failure rate. Where shape parameter <1.
(ii) Because of sporadic failures, the middle section has a steady failure rate. Where $m = 1$.
(iii) The final area shows a rising failure rate as the result of wear-out issues. Where shape parameter >1.

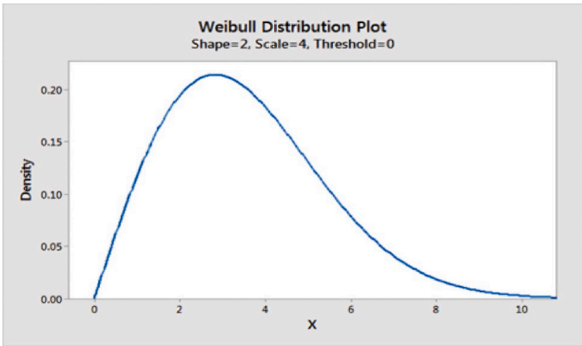

Fig. 4d. Typical Weibull distribution with shape parameter equal to 2 [121].

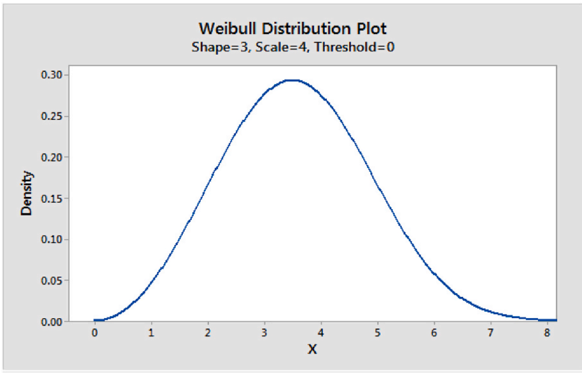

Fig. 4e. Typical Weibull distribution with shape parameters between 3 and 4 [116].

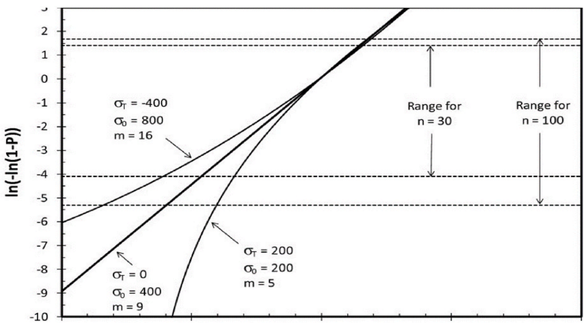

Fig. 4f. Typical Weibull distribution with shape parameter greater than 10 [117,124].

Not every product has a bathtub curve failure rate. A product is considered to follow the bathtub curve when early causes of potential failures, like manufacturing defects or damage received during transit, are identified and addressed. Throughout a product's midlife, failure rates are consistent. As a product age, wear out increases the failure rate. The life cycles of many consumer electronics goods exhibit the bathtub curve [115,127,128].

2.2. *Procedure for the 2-parameter Weibull analysis (2-PWA)*

The 2-parameter W_d serves as the foundation for Load and Resistance Factor Computations (LRFC). This method begins by applying a 2-parameter W_d to an entire data set or a subset of data in place of the distribution's lower end [120,129]. The W_d is categorized by two parameters: m (dimensionless) and x_0 (m/s) [130–132]. Several approaches to assessing Weibull parameters have been proposed by various researchers. Dodson [133] presented various procedures to evaluate the m (dimensionless) and x_0 (m/s), plus the highest probability estimator and likelihood plotting. The highest probability technique is suggested for ceramics [130]. The cumulative distribution function is denoted by Equation (1) stated above [130]. Fig. 6 is a typical 2-parameter Weibull plot.

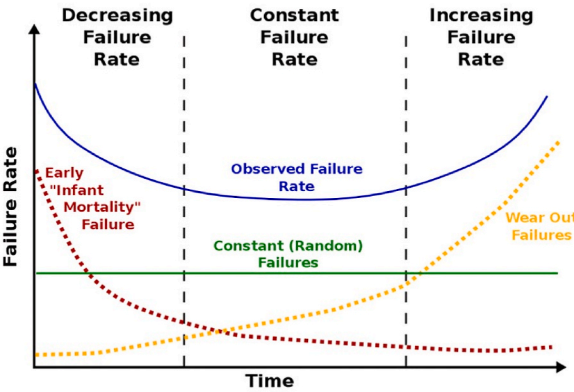

Fig. 5. A typical bathtub curve showing failure stages [125,126].

The Probability Density Function (PDF) is represented by equation (2) [130]:

$$P(x) = \frac{dP}{dx} = \frac{m}{xo}\left(\frac{x}{xo}\right)^{m-1} exp\left[-\left(\frac{x}{xo}\right)^{m}\right] \tag{2}$$

For two parameters only, Tiryakioğlu and Hudak [101] in a study presented a stepwise way of conducting Weibull analysis that depends upon the linear regression procedure, which is normally applied in the analysis of fracture value. In what follows, these steps are highlighted.

2.2.1. Allocate probability to Individually statistics point

Several probability estimators (alternatively referred to as simple rank-estimator functions) can be found in the literature [134–137]. For large data, the formula should be used according to Equation 3 (a) [135]:

$$P(x) = \frac{t - \mathrm{u}}{n + v} \tag{3a}$$

where t = ascending order rank, n = sample size, and u and v = empirical constants.

In reality, the plotting locations in equation 3 (b) and (c) below are generally used [138–143]:

$$P(x) = \frac{t - 3/8}{n + 1/4} \quad for\ n \geq 10 \tag{3b}$$

$$P(x) = \frac{\mathrm{t} - 1/2}{n} \quad for\ n \geq 11 \tag{3c}$$

Monte Carlo simulation investigations [144–150] disclosed that probability estimators yield partial evaluations of the Wm (the mean of predictable Weibull moduli) and are dissimilar from the factual Wm (model sizes (n) among 5 and 100). The extent of the bias rests on the values of *u* and *v* as well as the sample size. With a small number of statistics, other distributions, particularly the normal

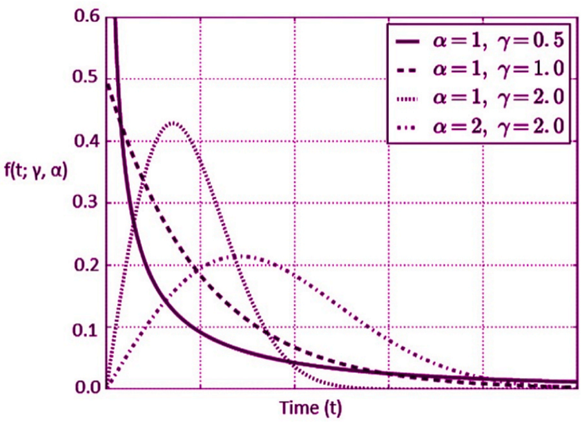

Fig. 6. Typical 2-parameter Weibull distribution plot [101,130].

distribution, resolve and possibly afford suitable turns. Monte Carlo simulation investigation is the commonly used method in probabilistic analysis in engineering. It is used to generate Weibull data points and for the validation of the reliability analysis and easy approximation of the analysis for the accuracy of the results [151–156]. Since it allows for operational or correlation-type interactions of the data being used, Monte Carlo simulation is significantly more flexible [157]. Also, for the estimation of standard errors [158–161]. it makes it easier to understand the multipart mathematical equations with accurate prediction [162–166].

2.2.2. Obtain linear regression fit

That is the plot of ln(x) against $\ln[-\ln(1-P)]$ [167]. The most frequently applied approach to solving the Weibull is the Weibull probability graph. Changing equation (1) to linear form, we have equation (4) [101]:

$$\ln[-\ln(1-P(x))] = m\ln(x) - m\ln(x_0) \tag{4}$$

From the above equation, m is the slope, and $m\ln(xo)$ is the intercept of the plot. Henceforth, the best-fit line for this probability plot signifies the linear regression way for assessing the two Weibull parameters (i.e., m = shape and x_0 = scale).

2.2.3. Conduct goodness-of-fit (GOF) test

A GOF test is a numerical trial that regulates whether the analysis figures trail the distribution model. If the figures excel in the GOF test, it proves that it trails the typical form thoroughly enough that forecasts can be decided and founded on that model. If the figures fail the GOF test, it shows that the figures do not trail the model thoroughly enough to make forecasts and that the figures do not look to trail a definite form [168–170]. Weibull outcomes are effective when GOF tests are fulfilled. GOF tests for a W_d comprise the following [171].

(i) R^2 [l]inear regression (least squares). If $R^2 > 0.9$, it is an acceptable fit for linear regression.
(ii) Kolmogorov-Smirnov: uses the confidence level and P-value to determine if the figure is a good fit.

If P > 1 - confidence level, the test passes [172].

The GOF of the Weibull design can also be evaluated using the straightness of the Weibull plot, according to Park et al. [173–176]. The sample correlation coefficient of the matching points can be used to determine the degree of linearity in the Weibull plot as shown in Equation (5) [101,176]:

$$\ln x, \ln[-\ln(1-P(x))] \tag{5}$$

Let: $U_x = \ln x$; $V_x = \ln[-\ln(1-P(x))]$; $\overline{U}_x = \frac{\sum Ux}{n}$ and $\overline{V}_x = \frac{\sum Vx}{n}$ [176]:

then; The sample correlation coefficient, R, from the plot, is denoted by Equation (6) [176]:

$$R = \frac{\sum_{i=1}^{n}(U_x - \overline{U}_x)(V_x - \overline{V}_x)}{\sqrt{\sum_{i=1}^{n}(U_x - \overline{U}_x)^2 . \sum_{i=1}^{n}(V_x - \overline{V}_x)^2}} \tag{6}$$

The application of a probability plot, nevertheless, is independent and inadequate, and so, it is assuredly suggested that probability plots are constantly supported by other GOF tests [177]. However, rich rules for the exploitation of R^2 as a GOF test have only recently been established by Tiryakioğlu et al. [178], who conducted Monte Carlo simulations to fix the points of R^2 at $x_0 = 0.05$ ($R^2_{0.05}$). Tiryakioğlu et al. stated that equation (7) may be applied for trial sizes between 5 and 100 [178]:

$$R^2_{0.05} = 1.0637 - \frac{0.4174}{n^{0.3}} \tag{7}$$

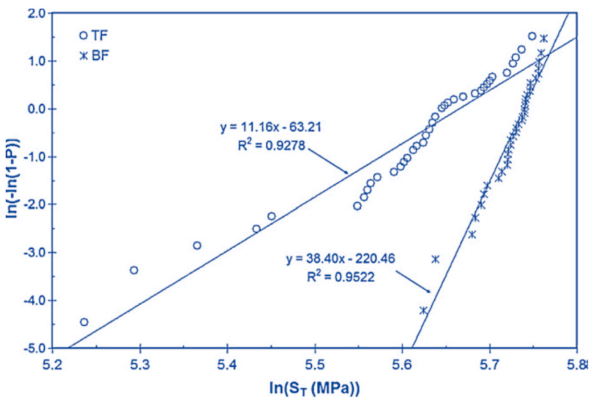

Fig. 7a. Typical Weibull graph for two samples [178].

The proposition that the statistical set trails the tried distribution is excluded once the p-value for the estimated $R^2 <$ a quantified data for the Category I error, which is characteristically set as 0.05. Otherwise, if the estimated $R^2 > R^2_{0.05}$, it can be resolved that the figure originates from a W_d. Hence, the WA must be rejected and stages 4.4 through 4.66 will not be engaged [178].

2.2.3.1. Real life examples. The real-life example here is two datasets reported by Ref. [178] that were used to show the application of the GOF methods suggested by the researchers. The two datasets were extracted from a study by Green and Campbell [179,180], who revealed that the tensile strength (TS) of alloys is influenced to a high degree in the mould-filling phase. If the mould is filled gently, TS is greater and has better reliability. On the other hand, tensile strength has a lesser average and greater unpredictability when the mould filling is intense. The two datasets exemplify these two kinds of mould filling: top-filled which is relatively intense, and bottom-filled, which is gentle. The mould filling sample size is 45 and 36 for top filling and bottom filling, respectively. For the graph point formula (equation (3c)), v is 0.481 and 0.466 for top filling and bottom filling, respectively, and u = 0 [181]. The Weibull probability plots are shown in Fig. 7a and the predictable parameters as well as goodness-of-fit measures are presented in Table 1.

For top fill, $R^2 < R^2_{0.05}$, signifying that the Weibull fit has to be unacceptable. It can be observed that in Fig. 7a, the slope for the last five points appears to be less when compared with other data. This variation in slope demonstrates a reliable instrument to estimate the GOF to the Weibull distribution. The important data for R^2 with $R^2 = 0.05$ ($R^2_{0.05}$) were estimated for each dataset size (Fig. 7b) using equation (7). The distribution of the mechanical testing data is Weibull if $R^2 \geq R^2_{0.05}$. Hence, they concluded that equation (7) be used for the GOF test [178].

2.2.4. Determine confidence intervals (CI) for the calculated Weibull parameters

It remains imperative to understand that the calculated Weibull parameters have their statistical distributions. Therefore, it is necessary to compute assurance intervals for the two Weibull parameters, particularly. The calculated Wm distribution does not trail at all in the prescribed distribution. Hence, the practice of percentage points is essential to estimate the confidence intervals. If the distribution of the projected scale parameter is normal, then the use of percentage point tables is not essential [181].

The standard deviation, S_{xo}, of the predictable scale parameter (after standardization) is computed using the probability estimators according to equation (8) [181]:

$$S_{xo} = \frac{0.359}{\sqrt{n}} \tag{8}$$

Thus, confidence intervals for the factual x_o can be gotten using equation (9):

$$\frac{\hat{x}_o}{1.000 + Z_{1-\frac{x_o}{2}} \cdot \frac{0.359}{\sqrt{n}}} \leq x_o \leq \frac{\hat{x}_o}{1.000 + Z_{\frac{x_o}{2}} \cdot \frac{0.359}{\sqrt{n}}} \tag{9}$$

Let α = 0.05 (95 % confidence), $Z_{1-\frac{x_o}{2}}$ and $Z_{\frac{x_o}{2}}$ are 1.96 and −1.96, respectively [101].

Let's examine the bottom fill data with n = 36, m = 38.4, and $\hat{x}_o = 311.4$ from the real-life example (subsection 2.2.3.1) to demonstrate how to evaluate the lower limit values. A single-side 99 % confidence interval, according to Ref. [181], occurs when $m >$ 26.6. Calculated from 38.4/1.446, the lower bound of a single-side 99 % confidence interval for $m = 1.446$. Equally, $\hat{x}_o > 273.4$ is the single-sided 99 % confidence interval for a neutral estimate for $\hat{x}_o$. The single-sided 97.5 % confidence interval for the population 10th percentile (P′ = 0.10) is found to be 0.60 when Inserting $m = 26.6$, $\hat{x}_o = 1.0$ is used.

Determining the confidence interval with results for the 10th percentile in Table 2 (Appendix A) of Ref [178], provides a 97.5 % confidence that the P* > 0.82. This means we are 97.5 % confident that 90 % of the population is > 0.82. In conclusion, different confidence intervals are added to get the final estimate. Thus, if $\hat{x}_o = 1.0$, then there is a 99 % confidence that m > 26.6 and we can be 97.5 % confident that the P* >0.82. In other words, when $\hat{x}_o = 1.0$, we are around 96 % (0.99 × 0.975) certain that the population's P* > 0.82. Furthermore, we can be around 95 % (0.96 × 0.99) convinced that the P* > 224.2 (273.4 × 0.82) because there is 99 % confidence that $\hat{x}_o > 273.4$.

2.2.5. Estimate lesser assured values

As soon as the Weibull parameters are known, it is necessary to get conventional estimates in design ideals, by calculating a certain percentile (pct) of the W_d [182]. To find a certain pct of the Weibull distribution, equation (1) can be reorganized to give equation (10) [101]:

$$x_p = x_o[-\ln(1-P)]^{\frac{1}{m}} \tag{10}$$

Table 1
Typical statistics of two Weibull data [178].

Serial	Samples	n	$R^2_{0.05}$)	m
1	Top Fill	45	0.9305	11.16
2	Bottom Fill	36	0.9213	38.40

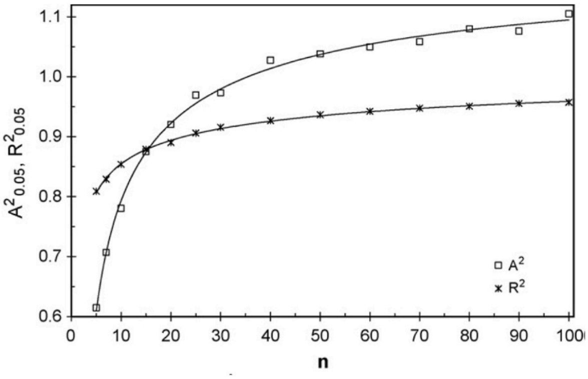

Fig. 7b. The important data of $R^2 = 0.05$ for model sizes between 5 and 100 [178].

where x_p is the P_{th} percentile. Since x_0 & m are unknown, corresponding approximations, $\hat{x}_o$ *and* $\hat{m}$ have to be applied to estimate the percentile. Because $\hat{x}_o$ *and* $\hat{m}$ have their distributions, the appraised percentiles will take a distribution, which is anticipated to be controlled by the distribution of $\hat{m}$, due to the weighty consequence of m on the percentile. Hudak and Tiryakioğlu [181] recently established a way to evaluate the percentiles of a W_d at a certain confidence level (CL). The authors presented tables for several sample sizes obtained from Monte Carlo simulations by substituting $x_o = 1$ and $m = 1$. When m is not equal to one (1), the pct (columns) for a certain CL (rows) is calculated by Equation (11.1) [181]:

$$P = 1 - exp\langle - \left\{ [- ln(1 - P')]^{\frac{1}{m}} \right\} \rangle \tag{11.1}$$

where $P^* =$ percentile of attention. For example, the authors in Ref. [181] studied a situation where $\widehat{m} = 3$; and n = 40 to compute the distribution for the 10th percentile. Using Equation (10), Putting $\widehat{m} = 3$; and $P' = 0.10$, the value of $P^* = 0.376$. This means that the distribution for the 37.6th pct when $\widehat{m} = 1$ and $m = 1$ gives the same result for the distribution as the tenth pct when $\widehat{m} = 1$ and $\widehat{m} = 3$. Afterwards, interpolation can be applied to evaluate the percentile standards (or values).

The failure probability $P_f(x)$ can also be found using Equation (11.2) [182–188]:

$$P_f(x) = \frac{a - 0.3}{N + 0.4} \tag{11.2}$$

Where N = Sum of trials; a = the failure sequential number, and P_f (x) is the failure probability.

The Coefficient of Deviation can be calculated as given in equation (11.3):

$$\Big/ CD \Big/ = \frac{S_d}{MTTF} \tag{11.3}$$

According to some researchers, Sd and MTTF can be calculated as given in equation (11.4) [189–192]:

$$Standard\ deviation, S_d = x_o \sqrt{\partial\left(1 + \frac{2}{m}\right) - \partial^2\left(1 + \frac{1}{m}\right)} \tag{11.4}$$

$\partial =$ *gamma function* and/CV/is the function of parameter m [1 93].

Also according to Equation (11.5) [193]:

$$\text{Mean Time to Failure (MTTF)} = x_o \partial\left(1 + \frac{1}{m}\right) \tag{11.5}$$

According to Equation (11.6) [193],

$$\text{Assume } m > 8, CV = \frac{1.2}{m} \tag{11.6}$$

Revol et al. [193] confirmed that the correlation $CV = 0.78/\sqrt{n}$ offered a perfect connection with experimental results. To identify an appropriate number of samples to produce a restricted variation of the anticipated strength, the influence of the fluctuation of m on the predicted value of strength was explored.

2.2.6. *Comparison of two Weibull moduli*

As the Wm has been applied as a degree of reliability of manufacturers, a proper process is essential to evaluate the Weibull moduli from two groups of manufacturers. The authors have recently presented the outcomes of their Monte Carlo simulations for weighing two Weibull moduli for sample scopes between 10 and 100. It was observed that 92.5 and 97.5 percent of the distributions for m_1/m_2, where $n_1 \geq n_2$. The values can be adopted to examine the proposition that the two Weibull moduli are equal at $x_o = 0.05$ [101] (Table 3, Appendix A).

2.3. Weibull Distribution for three-parameter

The reality of failures covers critical data around the firmness of the system. Particularly for very reliable systems, the application of this data to forecast a likely uncertainty is important. Uncertainty in a product can be viewed as an alteration of the dispersal of period among failures; the distribution may vary or a change may occur. These conditions can be detected using a statistical control plan [194–196]. Nevertheless, generalities of the exponential distribution (like Weibull and Gamma) are beneficial in showing reliability [197–205]. Three-parameter Weibull distributions are beneficial in the sense that their logic implies that verge parameters are considered in modelling [206–208]. This section will review the three-parameter Weibull Distribution.

Let $\beta = m$; $\alpha = x_o$ and $\gamma = y_o$, then; the PDF for the three-parameter Weibull distribution is denoted by Equation (12) [206,208]:

$$P(x;\ x_o, m, y_o) = 1 - exp\left\{-\left(\frac{x - y_o}{x_o}\right)^m\right\} \tag{12}$$

where $x_o > 0$ = scale parameter, $m > 0$ = shape parameter and $y_o < x$ = threshold parameter. Then Equation (13.1) gives the corresponding PDF [131,209,210]:

$$p(x;\ x_o, m, y_o) = \frac{m}{x_o}\left(\frac{x - y_o}{x_o}\right)^{m-1} exp\left\{-\left(\frac{x - y_o}{x_o}\right)^m\right\} \tag{13.1}$$

For an unknown shape parameter, $m,\ x_o, and\ y_o$, they have to be found by an iteration system because of uncontrollable nonlinear terms in the likelihood calculations. Ref [211] found clear modified maximum likelihood (MML) estimators of the threshold and scale parameters $y_o\ and\ x_o$ which are asymptotically equivalent to extreme probability estimators.

Using the first two terms in the Taylor series expansion they got the subsequent estimators given in equations (13.2)–(13.5) [212,213]:

$$\widehat{m} = \frac{T + \sqrt{T^2 + 4nZ}}{2\sqrt{n\,(n-1)}} \tag{13.2}$$

$$x_o = U + V\widehat{m} \tag{13.3}$$

where:

$$W_{(i)}^{-1} \cong \tau_{1i} - \rho_{1i} W_i, \tau_{1i} = 2k_{(i)}^{-1};\ \rho_{1i} = k_{(i)}^{-2};\ k_i = G\left(W_{(i)}\right)$$

$$W_{(i)}^{y_o-1} \cong \tau_{2i} + \rho_{2i} W_{(i)}, \tau_{2i} = (2 - y_o) k_{(i)}^{y_o-1}$$

$$\rho_{2i} = (y_o - 1) k_{(i)}^{y_o-2}, (1 \leq i \leq n)$$

$$t = (y_o - 1)\sum_{i=1}^{n} \rho_{1i} + y_o \sum_{i=1}^{n} \rho_{2i}$$

$$U = \frac{\left\{(y_o - 1)\sum_{i=1}^{n} \rho_{1i} + y_o \sum_{i=1}^{n} \rho_{2i} x_{(i)}\right\}}{t}$$

$$V = \frac{\left\{y_o \sum_{i=1}^{n} \tau_{2i} - (y_o - 1)\sum_{i=1}^{n} \tau_{1i}\right\}}{t}$$

$$T = y_o \sum_{i=1}^{n} \rho_{2i}\left(x_{(i)} - U\right) - (y_o - 1)\sum_{i=1}^{n} \rho_{1i}(x_i - U)$$

$$Z = (y_o - 1)\sum_{i=1}^{n} \rho_{1i}\left(x_{(i)} - U\right)^2 + y_o \sum_{i=1}^{n} \rho_{2i}(x_i - U)^2 \tag{13.4}$$

$$Note: k_i = G\left(W_{(i)}\right) \approx k_{(i)} \cong M^{-1}\left(i/(n+1)\right) \tag{13.5}$$

where $F^{-1}_{(x)}$ is known as the inverse distribution function for the 3-parameter W_d. Though the Fisher data matrix was applied to get asymptotic alterations and covariance as it occurs for $y_o > 2$, it is also possible to find the MML estimators for $1 < y_o < 2$ [214,215].

The symmetry settings are not fulfilled for the maximum likelihood (ML) estimate of the three-parameter Weibull distribution since the backing of the PDF rests on the unidentified parameter once the threshold parameter y_o is not known. The ML estimators may not be available at that point, and even if they are, they may not have the standard asymptotic properties [216–221]. Arising from this, several different procedures have been sought after in the literature. Different researchers have specified comprehensive explanations of several procedures for parameter estimation of the 3-parameter W_d [216–229]. For example, Ahmad [230], Juki'c et al. [231], and Markovic et al. [232] investigated several types of least-squares estimators for the three-parameter Weibull distributions. The least squares estimate (LSE) based on doubly Type-II censored samples was investigated by Nagatsuka [233]. Cousineau [234] provides a succinct overview of parameter estimation for a three-parameter Weibull distribution based on a full sample.

2.3.1. Estimation of the shape parameter, m

Moderately, limited approaches have been projected to evaluate the unidentified shape parameter, *m*, for the three-parameter Weibull distribution [235–237]. Sürücü & Sazak [194] used a calibration procedure [195] to determine *m* by estimating $\ln l$ of some values of m and the equivalent estimates $\widehat{x}_o$ *and* $\widehat{y}_o$ (which have unambiguous algebraic formulae), as given [238]:

$$V_{(x)} \cong \prod_{i=1}^{n} \frac{y_o}{\widehat{m}} \left(\frac{x_i - x_o}{\widehat{m}} \right)^{y_o - 1} exp\left\{ \left(\frac{x_{i-}\hat{x}_o}{\widehat{m}} \right)^{y_o} \right\} \tag{13.6}$$

$$x \geq x_o \; ; \; \widehat{m}, y_o \; > o$$

Tiku & Akkaya [238] estimated (Equation (13.6)) at points $y_o = i \times D, i = 0, 1, \ldots n \; and \; D = 0.1$. The statistics of y_o, which take full advantage of the likelihood role, will be the estimate for *m*. Sürücü & Sazak [194] recommend that since *m* affects the estimates for x_o *and* y_o, the early model width should be as large as possible (say, greater than or equal to 30) to get an appreciable evaluation of '*m*'. Some researchers noted that when x_o approaches the first-order statistic, the likelihood can tend to infinity which could result in inconsistent MLEs of the other two parameters. They suggested a fix regarding the possibility of solving this issue [239,240]. Using Monte Carlo simulations, different methods were adopted by Cousineau [228] to estimate the Weibull shape parameter.

To determine failure analysis measures, Shafiq et al. [241] employed an intelligent numerical computer solution that was reliant on artificial neural networks (ANN) (software). Using the software, the study investigates a dependability model based on the inverse power law model and the exponential Weibull distribution. Based on their findings, they came to the remarkable conclusion that when combined with the appropriate statistical model, ANNs can practically compute dependability metrics. In another study, a model of reliability designed on inverse power law and a generalized inverse Weibull model was proposed. The work gave a perfect structure for showing the effectiveness and functionality life cycle of equipment. It was observed that the valuation of the recommended distribution differs from the conventional model of inverse Weibull, and that impacts the average time to failure of the component considered [242]. In the study, reliability was modelled according to equation (14.1) [242]:

$$H_r = \frac{1}{kr^{\delta}} \tag{14.1}$$

where: Hr = Failure mean time; r = degree of stress; k = characteristic that can be influenced by design; and δ = *stress*:

It is feasible to show how different condition levels can affect the lifespan of equipment by using equation (14.2) [242].

$$f(x \setminus m, k, r, \delta) = \frac{1}{kr^{\delta}} m x^{-(m+1)} {x_o}^m \exp\left\{ - \frac{1}{kr^{\delta}} \left(\frac{x_o}{x} \right)^m \right\} \tag{14.2}$$

2.3.2. Models and hyperparameters in Weibull Distribution

Hyperparameters are parameters whose values dictate the model parameters that a learning algorithm ultimately learns and regulates the learning process. The prefix "hyper" implies that these are "top-level" parameters that govern the process of learning and the resulting model parameters [243–246]. Algorithms for machine learning (ML) have been applied extensively in many different fields and applications. An ML model's hyper-parameters need to be adjusted to suit it to various tasks. The performance of ML models is directly affected by the choice of optimal hyperparameter configuration. It frequently calls for in-depth familiarity with hyper-parameter optimization methods and ML algorithms [246]. A model is defined or represented by the model parameters [243].

Conversely, parameters are found inside the model. Because hyperparameters cannot be altered by the model when it is being trained or learned, they are referred to be extrinsic to the model [244]. Hyperparameters regulate the model's training process, whereas parameters enable the model to learn the rules from the data. Data is how parameters determine their values. Hyperparameters, on the other hand, do not get their values from data. Before training the model, they must be manually specified [245–249]. The importance of hyperparameters in ML includes: determining how any ML model turns out, and they aid in achieving this. It has a significant impact on how quickly any ML algorithm converges [250,251]. When optimizing hyperparameters, the set of hyperparameters is frequently chosen based on the generalization performance, or score, of a validation set after being fitted on a training set. Nevertheless, there's a chance that this process will overfit the hyperparameters to the validation set.

Reliability distribution and data-driven models are the two general categories into which failure estimation approaches for materials may be divided [252]. Based on the reliability model and the distribution of the equipment's entire life period, fault data, as well as other reliability information, the failure estimation technique is established. Then, using the statistical approach, the failure and error data are computationally investigated to calculate the equipment's reliability measurement [251]. The exponential distribution [253] and the Weibull distribution [49] are the two primary life distributions that are frequently utilized in material reliability estimation. Weibull distribution is commonly employed in the reliability modelling of materials [52]. The advantages of using a reliability model include a straightforward model, quick training times, and good predictive power; nevertheless, the method's fitting capabilities and prediction accuracy are limited in situations with irregular distributions and insufficient data [51].

The parameter calculation approaches in traditional statistics are frequently utilized to calculate the parameters of Weibull distribution. The usually used techniques include MLE, moment estimation, and the least square technique. Some researchers [254] related the features of the mentioned estimation techniques, and the results reveal that the value evaluated by the MLE technique can well equate to the real necessities. Hence, the tiny material failure data is processed using the maximum likelihood estimate technique.

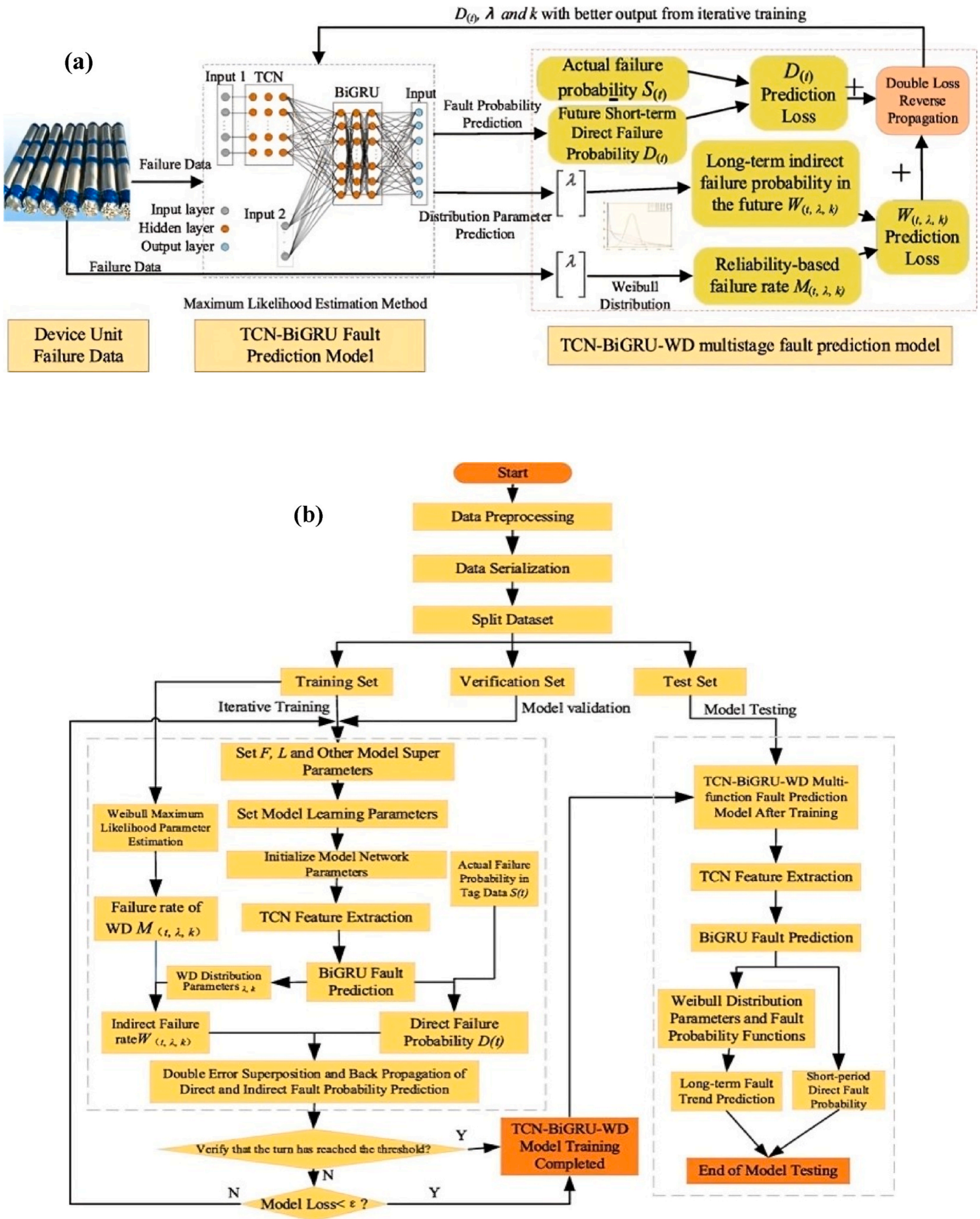

Fig. 8. A simple diagram for modelling in Weibull distribution (a) Plan and (b) ML Execution [51].

First, the Weibull distribution's shape parameter (m) and scale parameter (x_0) are taken into account. This method has the benefit of being able to predict the failure rate for a long period after the proper failure rate density function is identified; however, it has the disadvantage of requiring sufficient failure data and adhering to a particular distribution rule [51–53,254].

Deep learning is typically utilized in the data-driven modelling space to structure fault estimation models. Different researchers have recently used a variety of more advanced deep learning systems for fault prediction. To get around the LSTM model's poor training pace, Liu et al. [255] developed a Gated Recurrent Unit (GRU), which can achieve a higher convergence rate and produce prediction results that are comparable to the LSTM model. Wan et al. [256] suggested that a CNN architecture that excels at handling time series issues is the Temporal Convolutional Network (TCN). It addresses the "degradation" caused by the rise in network hierarchy and speeds up the feedback and convergence of deep networks through residual connectivity. Guo Ling et al. [257] used TCN to determine the distinctive characteristics of the time series data and then used the non-linear fit ability of the GRU neural network to create the TCN-GRU model to further improve the accuracy of prediction of time series data. Short-term forecasting derived from manufacturing load data shows that its estimation ability is notably more accurate compared to other point prediction models.

2.3.2.1. Hyperparameter model in Weibull Distribution. According to Ref. [51] the TCN side uses two hubs in the Weibull distribution fault estimation model to extract structures. Primarily the background involves level number (F) and lowest order length (L) in the hyperparameter (H). The volume of training parameters will rise if F is fixed large enough, which could cause the model to overfit and impair its performance. F may be set too small too in which case the model couldn't fit well and the extracted features might not be significant enough. L is the total of the convolution's lengths at and before the current point. The prior L-1 data and the current position make up the convolution data. An excessively large value for F contributes an excessive amount of information about the positions that came before it, which could result in more pointless calculations and less improvement in the model's efficiency. An excessively small value for F could result in insufficient prefix information being introduced and a decreased capacity to fit the model.

Orthogonal experiments adequately determine the proportions of both super-parameters. For example, to create a two-component, four-level experiment, F and L, the two orthogonal experiment factors, establish an array of parameters for each factor based on experience [258]. They then choose four suitable discrete values from the range. L needs to be an odd number to guarantee a fixed convolution centre anchor location [259]. A simple diagram for modelling in Weibull distribution is given in Fig. 8 (a) and (b). Adjust the model's learning parameters based on the level and design considerations. By varying the convolution layer F and sequence length L values, many fault prediction models are constructed. The accuracy and recall rate on the validation set are utilized as test results to assess the suitability of the parameter combination [51].

2.4. Weibull Modulus for different ceramics materials

In materials science, Weibull analysis was initially used almost solely for ceramics and glasses [260–262]. The unpredictability in measured material strength of brittle materials is defined by the dimensionless Weibull modulus, a parameter of the Weibull distribution [263–267]. In this scenario, the Weibull distribution model's form parameter, the Weibull modulus, accounts for the likelihood of a component failing under different loads. One should exercise caution when relying on the precision of the Weibull moduli that are obtained from a small number of tests. The Weibull modulus and its physical effects on the statistical distribution of fracture strengths in brittle materials have been estimated in several ways. For example, the theoretical value of the Weibull modulus labelling the dispersion in fracture toughness is proven to be a constant, i.e., Weibull modulus $(m) = 4$ [268], under the assumption that the fracture probability is proportionate to the volume of a fracture progression region in a brittle material. The application of fractal theory has revealed a relationship between the Weibull modulus, fractal dimension, and $m < 6$ in highly fractured rocks [30,269–271]. Weibull modulus elaborates on the mechanical behaviours of materials [70,269].

A higher m value suggested a narrower range of fracture stresses and a higher dependability/reliability because the m value represented the degree of variation in the strength of the tested samples [272–274]. Table 4 lists the typical values of the m for a few materials, such as bulk metallic glasses based on magnesium which were compiled.

2.5. Summary of steps in Weibull Distribution and its benefits

Brittle materials are widely characterized in the biomedical sector by Weibull statistics [281,282]. Ceramics, particularly high-performance ceramics like alumina, zirconia, or HAp, are routinely examined using the Weibull modulus (m) to ensure the consistency and dependability of their structure. Despite the rather robust probabilistic criterion for using the Weibull distribution for

Table 4
Weibull modulus values for certain materials

S/N	Material	Weibull Modulus, m	References
1	Local ceramics (Chalk, Brick, Pottery)	>2	[275,276]
2	Advanced ceramics (Al_2O_3, HAp, SiC)	≤ 10	[275,277]
3	Mg glass	>40	[277,278]
4	Glass Ceramics	<7	[279]
5	Zirconia	<7	[280]
6	Graphite	<13	[280]

brittle materials, an appropriately uncomfortable parameter estimate made its practical implementation difficult [281,283]. Much progress has been made recently in terms of making the Weibull distribution accessible. Elastic general-purpose statistical models exist that can be used to calculate the two-parameter Weibull distribution utilizing least squares (LS) or maximum likelihood (ML) approaches, or both [284–286]. A number of them offer tests for parameter variation among factor levels, appropriate probability graphs, and 95 % confidence intervals for the Weibull parameters. Additionally, a free open-source Excel calculator that facilitates a computerized LS calculation of Weibull parameters and the associated 95 % CI is available [287]. Despite this outstanding advancement, data analysis is still a source of unpredictability [288].

In summary, WA has the following advantages [289–291]: (a) It can be used to describe the data of materials without the restrictions of a pre-defined distribution hypothesis because it is robust enough to assume a variety of various distributions, such as the normal, exponential, and beta distributions. (b) The parameters $m,\ x_{o,}\ and\ y_o$ predict the distribution's index rate(s). (c) The analysis can deliver precise performance analysis and risk predictions even with very tiny samples.

The steps for WA using a worksheet (MS Excel) can be summarized as given [291].

1. Production of the materials and preparing the samples for mechanical testing
2. Collection of the data
3. Ranking of data in ascending order for the plots
4. Calculating the PDF $(\ln x, \ln[-\ln(1 - P(x))])$ for the distribution and plotting of the graphs
5. Determine the m and other parameters

2.6. Monte Carlo simulation

A popular way for assessing the performance of statistical methods is Monte Carlo simulation. When paired with trials, Monte Carlo simulations prove to be a very helpful tool for forecasting the dependability of different estimate techniques and their optimization [284,292]. It comprises generating random numbers (strength data) for a particular modulus (m) and character strength in the framework of the two-parameter Weibull distribution. It is certain that the basic Weibull sampling distribution assumption holds and that the precise parameter values (m, x_o) of this distribution are known thanks to the utilization of Monte Carlo techniques. This kind of technique has several benefits [287,292].

1. Real experiments do not need to be conducted to create strength information based on a Weibull distribution using specific parameters m and x_o
2. Parameter values are freely selectable; for example, they can be set to values often noticed in dental material research.
3. The number of samples can be arbitrarily adjusted and as many results as desired can be obtained.
4. A statistical method can be used in the same manner as measured data to analyze a particular simulated sample.

On the other hand, estimations of parameters generated from the simulated sample ($\dot{m}$,$\dot{x_o}$) could be juxtaposed to the observed true values (m, s) to assess the statistical technique's effectiveness in terms of relative error and bias, unlike measured data [287].

2.7. Case study: related works on the application of Weibull analysis on HAp and related materials

In a Weibull modulus analysis, the samples should be cracked with a standard test procedure like the 4-point bend test or a biaxial flexure test [293–295]. Weibull Analysis has been extensively adopted to analyze the failures in an estimated property, such as fracture strength [296,297]. Consequently, the Weibull Modulus, m is directly connected to the material's reliability. Naturally, WA is carried out on a set of samples that are supposedly alike. Aguirre et al. [26] reinforced HAp with boron nitride platelets to increase the fracture toughness of the HAp samples and achieved 2.3 MPa $m^{1/2}$ and 79.79 MPa for fracture toughness and flexural strength, respectively. The Weibull distribution showed a low failure probability and a safety factor. The factor of Safety (FOS) = Yield Stress/Working Stress. If the FOS = 1, then it signifies that the design load = to the safety load [298,299]. Abifarin et al. [300] considered a two-parameter Weibull distribution on the mechanical properties of HAp to ascertain the reliability of the produced scaffold.

The fracture toughness, flexural strength, compressive, and hardness data/statistics can be analyzed with the aid of the Weibull probability density function (PDF). Equation (2) and the probability of failure, P(x), for a sample under a given stress can be calculated using the Weibull cumulative distribution function (CDF): equation (1) [301–308]. Notwithstanding the usefulness of the m, as a measure of the mechanical reliability of brittle materials, there is little research on m for porous HAp [293]. It has long been acknowledged that there is a strong relationship between strength and flaw distribution. The extent of its impact on strength is one implication of statistical strength behaviour in brittle materials. Its continued existence has been predicted hypothetically [308–310] and shown in numerous exploratory trials [148,311]. Using WA, the reliability of a ceramic material like HAp can be predicted.

In another study by Fan et al. [66], m was estimated for 441 sintered HAp samples cracked in biaxial flexure for $0.08 \le P \le 0.62$. The m against P graph was "U-shaped" with a varied band of m data for $P < 0.1$ (Area 1) and $P > 0.55$ (Area 3), and a thinner band of m data in the transitional porosity area of $0.1 < P < 0.55$ (Area 2). The restricted array of m ($\sim 4 < m < 11$) in Area 2 has vital inferences as Area 2 comprises the P array for the majority of the uses of porous brittle materials. The grain size versus density path of the HAp samples revealed a distinct value with limited grain development for samples with relative densities of less than about 0.8–0.9. Fig. 9 is a typical Weibull plot as given by Fan et al. Ćurković et al. [55] used Weibull analysis to investigate the flexural strength of alumina ceramics. The three-point bend test was used to determine the flexural strength of standard purity alumina ceramics. Flexural strength has been determined to be between 266.7 and 357.5 MPa. The numerical unpredictability of flexural strength calculated by the three-point bend test was investigated using a two-parameter Wd function. Flexural strength was measured at 17.4 Wm. This restriction can be used to characterize the variability in the tested material's flexural strength as well as its consistency.

Nevarez-Rascon et al. [312] investigated the inconsistency in mechanical properties of a nanocomposite using Weibull statistics. Uniaxial compression examinations at room temperature of specimens 6.35 ± 0.03 mm in diameter and 12.50 ± 0.63 mm in length and Vickers hardness readings on polished surfaces were conducted. The indentation fracture toughness (K_{IC}) was obtained from the average crack length and WA was made on the statistics. The ATZ2 (18.0 wt % Al_2O_3 + 2.0 wt % (w) + 80.0 wt % ZrO_2 (TZ-3Y)) nanocomposite gave the maximum average compressive load of 1200 MPa, the maximum data of distinctive strength, σ_o, of 1340 MPa with *m* of 3.25 and moderately high fracture toughness (4.7 ± 0.7 MPa $m^{1/2}$), signifying that with the wide variety of mechanical properties gotten in the study, the material is characterized by diverse dental usages. However, zigzagged cracks were observed. In the two composites, the fracture shape was a mixture of transgranular and intergranular fractures [313–316]. The notch of intergranular fracture rises with the growing Al_2O_3 content leading to low fracture toughness.

A 3D-printed HAp scaffold's dependability was predicted with the aid of Weibull analysis using compressive strength values [317]. With a correlation coefficient (R^2) above 0.90, the Weibull plots demonstrated good linearity (Fig. 10 (a) – (d)) [317]. All the scaffolds had a survival probability greater than 90 %. In their work, the highest value of *m* obtained was 1.0 [317,318].

Isaacson et al. [319] performed a compressive failure of porous gyroid scaffolds. The Weibull moduli of the scaffolds were discovered to be self-reinforcing, therefore initial failures brought on by minor manufacturing irregularities didn't seem to be the main reason for the scaffold's early catastrophe. HAp was reinforced with graphene and silver for dental applications. The Weibull analysis was used to determine the reliability of the binding strength to dentin. Four samples were tested and the obtained Weibull modulus ranged from 2.0 to 3.4. The Weibull plots are presented in Fig. 11 [320]. Using Mussel shells, Galotta et al. [321] produced nanocrystalline HAp. A Weibull Modulus of 9.1 was obtained for the HAp sample. D'Andrea et al. [322] produced HAp via the photopolymerization process and the mechanical reliability of ceramic scaffolds was assessed using the Weibull modulus. For the estimation of the Weibull modulus, strength information from the cantilever and notched beams was combined. The Weibull modulus was determined as the slope of the linear fit of the data. From the plot, the obtained *m* at 143 MPa was 2.6. The value of *m* can be improved by post-sintering surface machining which removes or strappingly decreases surface defects [323]. The assessment of a novel commercially obtainable ion-releasing HAp and their connections to establish anti-carcinogenic sources was done by Marovic et al. The reliability of the material was evaluated using WA. The result showed that the glass ionomer had the highest water sorption and the least predictable distribution of mechanical characteristics or properties [324].

Zhao et al. [325] performed the Weibull analysis of carbon-fibre-reinforced HAp composites. Huang et al. added HAp nanowires to produce an insulation network. Weibull modulus of 2.65 was obtained for the reliability analysis [326]. Karimi & Paydar [327] studied an anode electrode's fracture pattern and mechanical performance for solid use. Porosity and compressive strength measurements were between 59 and 75 % and 2.7 and 14.02 MPa, respectively. The Weibull study revealed a direct correlation between the Weibull modulus and cooling rate. Using quasi-static and high strain rates, an experiment was conducted to assess the transverse tensile strength of red deer. There was an 83 MPa improvement in tensile strength. The WA revealed that the osteo progress trend had greater tensile ductility than the osteon progress trend's transverse [328]. Przystupa [329] evaluated the reliability and durability of the coating surfaces of roofing materials. Higher shape and scale parameters were obtained which meant higher durability and reliability of the materials. Par et al. studied the flexural behaviour of an experimental composite. Flexural strength and modulus were appraised using a three-point bending test and WA was done to estimate material reliability. A higher Weibull modulus of 5.0 was obtained, signifying that the material is reliable for the intended applications [330].

Monteiro et al. [331] investigated the bond strength of various ceramic and dental materials to estimate the reliability of the merged edges. WA was executed to find the probability of failure (POF), Weibull modulus (*m*), and characteristic strength (CSS). At a bond strength of 24.88 MPa lower POF, greater *m*, and greater CSS were obtained. The highest data were obtained at 20.07 MPa. Lira et al. [332] studied the WA of fibre supports diluted with diverse cement forms and mechanically aged. Weibull behaviour strength of the materials was considerably high. The effect of laser sintering was observed to advance the bioactivity of a modified HAp. The

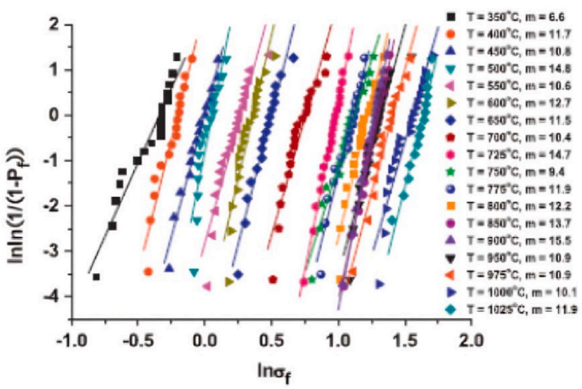

Fig. 9. Typical Weibull plot of HAp at different temperatures [66].

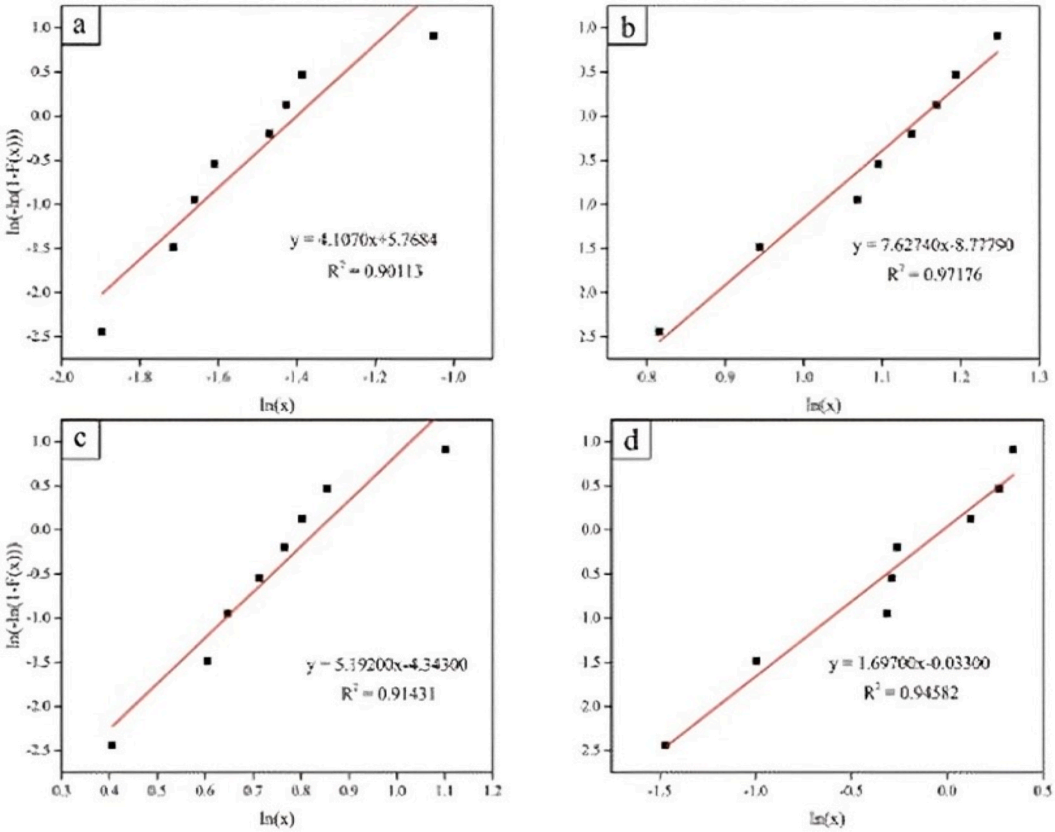

Fig. 10. Typical Weibull plots of 3D printed HAp [317].

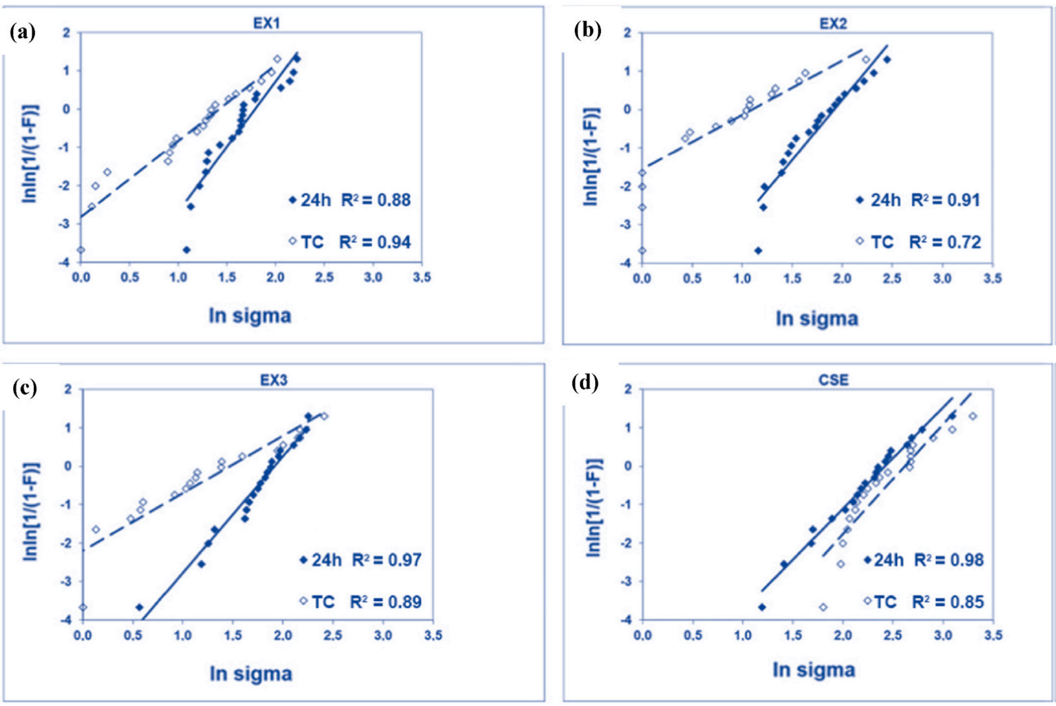

Fig. 11. Typical Weibull plots of reinforced HAp [320].

bioactive coat's reliability was inveterated by severe high-energy ultrasonic cavitation experiments and friction experiments against bovine bone, indicating no transferal of HAp to the bone. Additionally, WA was done to establish the changeability of the documented strength figures for every set. Equation (1) was employed to compute the Weibull modulus, *m*. The results showed a higher value of the *m* which points to larger homogeneity in the obtained strength values of the set [333]. Ilie [334] compared the manner contemporary resin-based composites react to mechanical stress associated with the tooth structure they are intended to substitute. WA was performed to determine the value of *m* and 5.2 was obtained.

Liao et al. [335] employed equation (4) in determining the reliability of a metallic glass wire and a Weibull modulus of 81.0 was obtained. They concluded that the Weibull modulus *m* reveals the reliability of the material's samples and a higher *m* value signifies a narrow distribution of the fracture strength and thus higher reliability. For the reliability analysis of metallic glass fibres, Liu et al. [336] performed two and three – Weibull analyses. They obtained *m* values of 5.71, 3.73, 4.27, & 4.03 and 3.36, 2.07, 2.10, &2.30 for the two and three Weibull analyses respectively. In another study by Wang et al. [337], the WA was used to obtain the Weibull modulus *m* of an amorphous alloy with a special structure and the value of *m* represented the dissemination range of the fracture strength of the material.

In a related study, we extracted HAp from bovine and catfish bones to synthesize a novel mix of HAp that can be useful for biomedical applications [69–74,82,338,339]. The samples were prepared and the compressive test was performed using a Universal Testing Machine. After completing the compressive strength tests, equation (4) was used to determine the strength values of the produced HAp samples, Plotting ln (ln (1/survival probability or the median rank) versus ln (compressive strength, x_0) produced the distinctive Weibull modulus and distribution. The results showed that the novel combination of these powders is a good and promising biomaterial for high-strength biomedical applications. Examining the correlation between the characteristic compressive strength and the Weibull modulus (*m*), a higher *m* was obtained for all the samples indicating a more favourable test design [82]. Sample C100 had the highest value of *m* (5.29) with a standard deviation of 0.92, while sample B75/C25 had the lowest value of *m* (2.67) with a standard deviation of 1.0. The high value of *m* ($m > 1$) indicates the materials might not fail in their early stage when relating the obtained *m* value with the bathtub [283,340]. Fig. 12 depicts the procedures employed in the production of the HAp samples and the WA of the novel mixture of HAp. The generated scaffolds are somewhat reliable by the acquired results, making them appropriate for use in biological fields. The Weibull plots from the work are presented in Fig. 13.

3. Conclusion and Future works

In this paper, we have reviewed the steps in Weibull distribution to critically analyze the strength data of brittle materials, such as ceramics and related materials. The WA and the steps for the analysis were highlighted. With the aid of WA, the *m* of the samples can be investigated to predict their failure rates. From the review, it was discovered that Weibull distribution is proven to confer to the feeblest-link concept. For brittle materials, the literature revealed that environs, production processes, and comparative factors are well-thought-out contributing factors for reliability. The Weibull modulus and characteristic strength from the analyses are appropriate in many circumstances, but it should be noted that they are estimations. The literature can provide confidence limits or uncertainty for these estimates. As the number of specimens increases to 10 or more, estimations of the characteristic strength quickly

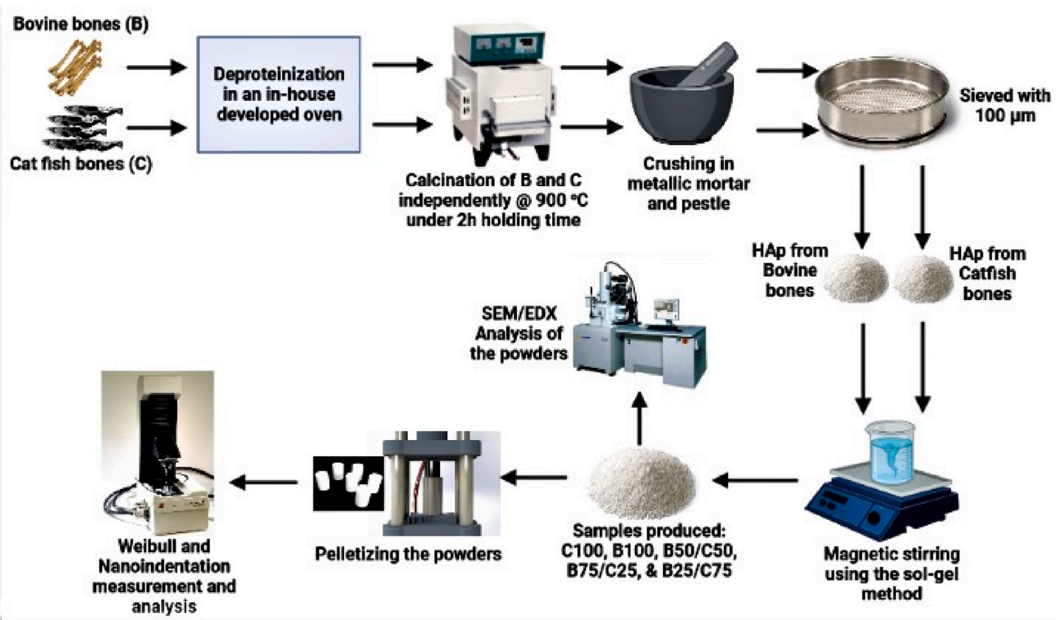

Fig. 12. Schematic details of the synthesis, characterization, and computational procedures [82].

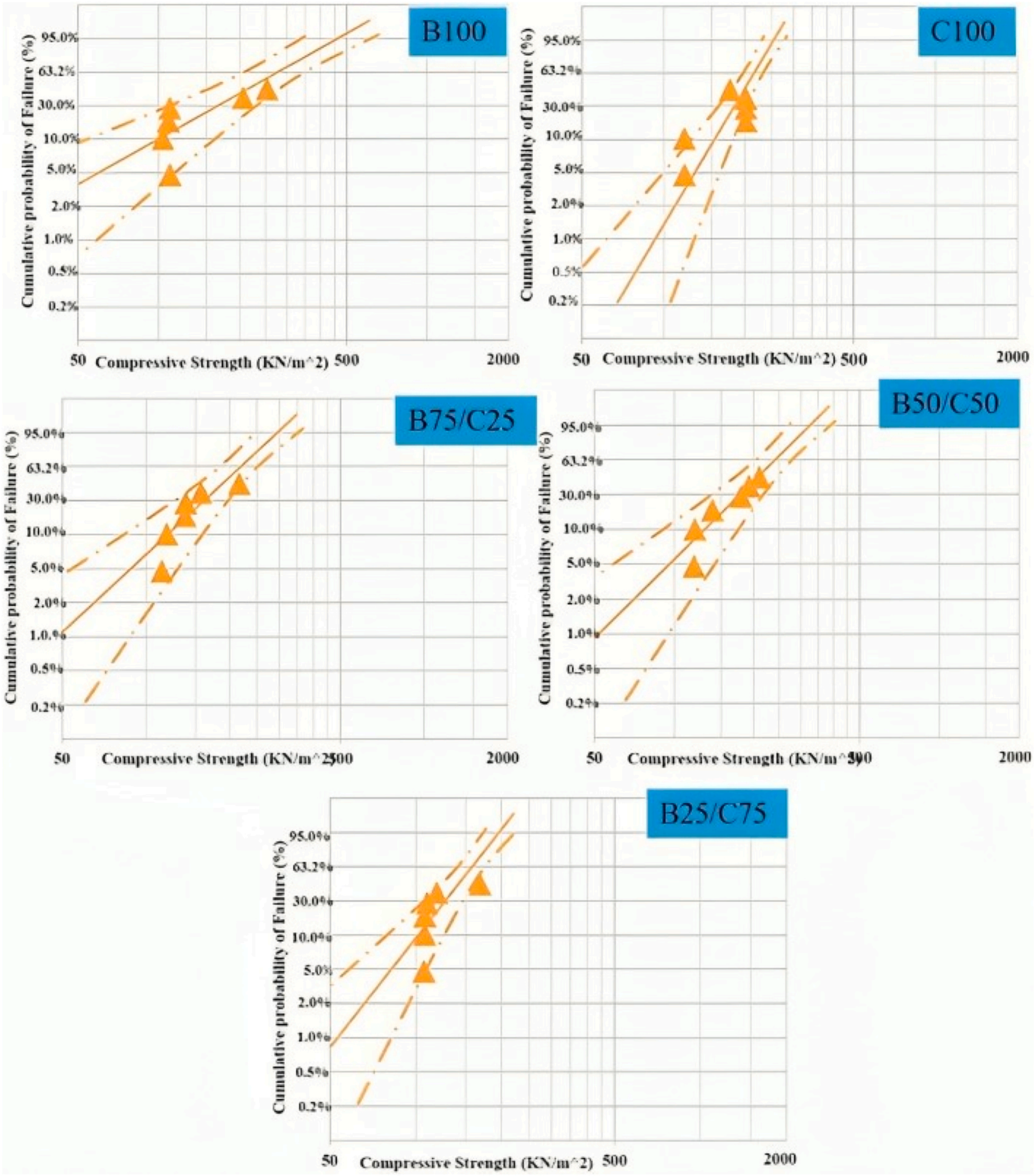

Fig. 13. Weibull plots of hydroxyapatite with high m [82].

converge on population values. Weibull modulus estimations, on the other hand, can vary when the sample set contains only a small number of test specimens or when the data does not fall on a single line. To acquire good estimations of the Weibull modulus, at least 10 test specimens, preferably thirty, are often required.

Abbreviations

ANN	Artificial Neural Network
CI	Confidence Interval
GRU	Gated Recurrent Unit
GOF	Good-of-Fit
HAp	Hydroxyapatite
LRFC	Load and Resistance Factor Computations
MLEs	Maximum Likelihood Estimators
MLs	Maximum Likelihoods
ML	Machine Learning
PC	Performance Characteristics
PDF	Probability Density Function
TCN	Temporal Convolutional Network
WA	Weibull Analysis

Funding

This research/literature review did not receive funding from any organization or individual.

4. Data availability

This is a review paper. No raw data was used.

CRediT authorship contribution statement

Obinna Anayo Osuchukwu: Writing – original draft, Visualization, Validation, Project administration, Methodology, Conceptualization. **Abdu Salihi:** Writing – review & editing, Project administration. **Abdullahi Ibrahim:** Visualization, Supervision. **Adamu Abdullahi Audu:** Validation, Supervision. **Mahdi Makoyo:** Investigation. **Sikiru Adepoju Mohammed:** Methodology, Investigation. **Mohammed Y. Lawal:** Methodology, Investigation. **Precious Osayamen Etinosa:** Writing – review & editing, Resources. **Ibitoye Opeyemi Isaac:** Visualization, Validation. **Peter Gbenga Oni:** Methodology. **Oreoluwa Gabriel Oginni:** Writing – review & editing, Investigation. **David Olubiyi Obada:** Writing – review & editing, Supervision, Methodology, Formal analysis, Conceptualization.

Declaration of competing interest

The authors declare that they have no known competing financial interests or personal relationships that could have appeared to influence the work reported in this paper.

APPENDIX A. TYPICAL WEIBULL RESULTS

Table 2
Typical Weibull fits of two values [178].

Data Set	n	Plotting Position		Parameter Estimates		Goodness - of Fit			*m*		95 % CL	
		u	v	*m*	x_o (MPa)	$R^2$0.05	R^2	Weibull Confirmation			x_o (MPa)	
TF	45	0.481	0	11.16	288.3	0.931	0.928	Not Agreed				
BF	36	0.466	0	38.40	311.4	0.921	0.952	Agreed	28.16	55.36	278.7	352.8
BFmod	37	0.468	0	50.71	279.7	0.922	0.980	Agreed	37.34	72.73	250.7	316.3

Table 3
A Table showing two Moduli [101].

n2	n1																								
	10		**15**		**20**		**25**		**30**		**35**		**40**		**50**		**60**		**70**		**80**		**90**		**100**
	0.412	2.434	2.262	0.475	2.222	0.488	2.151	0.494	2.124	0.505	2.100	0.507	2.089	0.517	2.058	0.524	2.049	0.535	2.042	0.534	2.027	0.536	2.011	0.540	2.030
		0.489	2.069	0.511	1.976	0.531	1.951	0.543	1.906	0.550	1.881	0.559	1.877	0.574	1.854	0.581	1.827	0.591	1.821	0.594	1.823	0.599	1.798	0.595	1.798
				0.526	1.889	0.553	1.851	0.571	1.799	0.575	1.798	0.585	1.767	0.600	1.722	0.609	1.708	0.614	1.703	0.621	1.690	0.629	1.693	0.629	1.693
						0.567	1.771	0.581	1.728	0.598	1.720	0.599	1.677	0.615	1.661	0.624	1.647	0.632	1.630	0.639	1.620	0.644	1.618	0.649	1.600
								0.596	1.677	0.608	1.662	0.621	1.622	0.634	1.612	0.643	1.597	0.653	1.583	0.660	1.573	0.661	1.559	0.668	1.549
										0.614	1.624	0.623	1.605	0.643	1.568	0.658	1.560	0.671	1.545	0.674	1.523	0.683	1.516	0.684	1.505
												0.636	1.569	0.655	1.552	0.668	1.531	0.674	1.515	0.685	1.510	0.693	1.492	0.694	1.489
														0.665	1.504	0.678	1.483	0.689	1.466	0.694	1.458	0.702	1.447	0.708	1.432
																0.690	1.444	0.702	1.439	0.709	1.420	0.713	1.412	0.721	1.402
																		0.710	1.415	0.714	1.399	0.724	1.389	0.731	1.380
																				0.722	1.384	0.731	1.382	0.739	1.360
																						0.737	1.361	0.741	1.355
—																								0.752	1.331

References

[1] Z. Wan, P. Zhang, Y. Liu, L. Lv, Y. Zhou, Four-dimensional bioprinting: current developments and applications in bone tissue engineering, Acta Biomater. 101 (2020) 26–42, https://doi.org/10.1016/j.actbio.2019.10.038.

[2] W. Wang, K.W. Yeung, Bone grafts and biomaterials substitutes for bone defect repair: a review, Bioact. Mater. 2 (4) (2017) 224–247, https://doi.org/10.1016/j.bioactmat.2017.05.007.

[3] S. Wu, X. Liu, K.W. Yeung, C. Liu, X. Yang, Biomimetic porous scaffolds for bone tissue engineering, Mater. Sci. Eng. R Rep. 80 (2014) 1–36, https://doi.org/10.1016/j.mser.2014.04.001.

[4] A.A. John, S.K. Jaganathan, E. Supriyanto, A. Manikandan, Surface modification of titanium and its alloys for the enhancement of osseointegration in orthopaedics, Curr. Sci. (2016) 1003–1015. https://www.jstor.org/stable/24908502.

[5] A. Jemat, M.J. Ghazali, M. Razali, Y. Otsuka, Surface modifications and their effects on titanium dental implants, BioMed Res. Int. 2015 (2015), https://doi.org/10.1155/2015/791725.

[6] H.S. Hedia, N. Fouda, A new design of dental implant coating using functionally graded material, Mater. Test. 55 (10) (2013) 765–771, https://doi.org/10.3139/120.110499.

[7] S.A. Asiri, H.S. Hedia, N. Fouda, Improving the performance of cementless knee prosthesis coating through functionally graded material, Mater. Test. 58 (11–12) (2016) 939–945, https://doi.org/10.3139/120.110942.

[8] S.M. Aldousari, N. Fouda, H.S. Hedia, F.W. AlThobiani, Comparison of titanium and FGM dental implants with different coating types, Mater. Test. 60 (2) (2018) 142–148, https://doi.org/10.3139/120.111133.

[9] D. Apostu, O. Lucaciu, C. Berce, D. Lucaciu, D. Cosma, Current methods of preventing aseptic loosening and improving osseointegration of titanium implants in cementless total hip arthroplasty: a review, J. Int. Med. Res. 46 (6) (2018) 2104–2119, https://doi.org/10.1177/0300060517732697.

[10] S. Awasthi, S.K. Pandey, E. Arunan, C. Srivastava, A review on hydroxyapatite coatings for the biomedical applications: experimental and theoretical perspectives, J. Mater. Chem. B 9 (2) (2021) 228–249, https://doi.org/10.1039/D0TB02407D.

[11] M. Figueiredo, A. Fernando, G. Martins, J. Freitas, F. Judas, H. Figueiredo, Effect of the calcination temperature on the composition and microstructure of hydroxyapatite derived from human and animal bone, Ceram. Int. 36 (8) (2010) 2383–2393, https://doi.org/10.1016/j.ceramint.2010.07.016.

[12] P. Kamalanathan, S. Ramesh, L.T. Bang, A. Niakan, C.Y. Tan, J. Purbolaksono, W.D. Teng, Synthesis and sintering of hydroxyapatite derived from eggshells as a calcium precursor, Ceram. Int. 40 (10) (2014) 16349–16359, https://doi.org/10.1016/j.ceramint.2014.07.074.

[13] A. Niakan, S. Ramesh, S.V. Naveen, S. Mohan, T. Kamarul, Osteogenic priming potential of bovine hydroxyapatite sintered at different temperatures for tissue engineering applications, Mater. Lett. 197 (2017) 83–86, https://doi.org/10.1016/j.matlet.2017.03.057.

[14] H. Abukawa, M. Papadaki, M. Abulikemu, J. Leaf, J.P. Vacanti, L.B. Kaban, M.J. Troulis, The engineering of craniofacial tissues in the laboratory: a review of biomaterials for scaffolds and implant coatings, Dental Clinics 50 (2) (2006) 205–216, https://doi.org/10.1016/j.cden.2005.11.006.

[15] J.K. Abifarin, D.O. Obada, E.T. Dauda, D. Dodoo-Arhin, Experimental data on the characterization of hydroxyapatite synthesized from biowastes, Data Brief 26 (2019) 104485, https://doi.org/10.1016/j.dib.2019.104485.

[16] D.O. Obada, E.T. Dauda, J.K. Abifarin, D. Dodoo-Arhin, N.D. Bansod, Mechanical properties of natural hydroxyapatite using low cold compaction pressure: effect of sintering temperature, Mater. Chem. Phys. 239 (2020) 122099, https://doi.org/10.1016/j.matchemphys.2019.122099.

[17] A. Niakan, S. Ramesh, P. Ganesan, C.Y. Tan, J. Purbolaksono, H. Chandran, W.D. Teng, Sintering behaviour of natural porous hydroxyapatite derived from bovine bone, Ceram. Int. 41 (2) (2015) 3024–3029, https://doi.org/10.1016/j.ceramint.2014.10.138.

[18] T. Goto, K. Sasaki, Effects of trace elements in fish bones on crystal characteristics of hydroxyapatite obtained by calcination, Ceram. Int. 40 (7) (2014) 10777–10785, https://doi.org/10.1016/j.ceramint.2014.03.067.

[19] A. Pal, S. Paul, A.R. Choudhury, V.K. Balla, M. Das, A. Sinha, Synthesis of hydroxyapatite from Lates calcarifer fish bone for biomedical applications, Mater. Lett. 203 (2017) 89–92, https://doi.org/10.1016/j.matlet.2017.05.103.

[20] C.F. Ramirez-Gutierrez, S.M. Londoño-Restrepo, A. Del Real, M.A. Mondragón, M.E. Rodriguez-García, Effect of the temperature and sintering time on the thermal, structural, morphological, and vibrational properties of hydroxyapatite derived from pig bone, Ceram. Int. 43 (10) (2017) 7552–7559, https://doi.org/10.1016/j.ceramint.2017.03.046.

[21] S. Ramesh, A.N. Natasha, C.Y. Tan, L.T. Bang, C.Y. Ching, H. Chandran, Direct conversion of eggshell to hydroxyapatite ceramic by a sintering method, Ceram. Int. 42 (6) (2016) 7824–7829, https://doi.org/10.1016/j.ceramint.2016.02.015.

[22] E.J.M. Edralin, J.L. Garcia, F.M. dela Rosa, E.R. Punzalan, Sonochemical synthesis, characterization and photocatalytic properties of hydroxyapatite nano-rods derived from mussel shells, Mater. Lett. 196 (2017) 33–36, https://doi.org/10.1016/j.matlet.2017.03.016.

[23] A.N. Klein, H. Zoz, N. Vicente Jr, U.U. Gomes, Advanced powder Technology X, Adv. Powder Technol. X (2017) 1–604.

[24] T. Laonapakul, Synthesis of hydroxyapatite from biogenic wastes, Engineering and Applied Science Research 42 (3) (2015) 269–275. https://ph01.tci-thaijo.org/index.php/easr/article/view/38306.

[25] M. Espanol, R.A. Pérez, E.B. Montufar, M.P. Ginebra, Ceramics. *Biomimetic, Bioresponsive, and Bioactive Materials: an Introduction To Integrating Materials With Tissues*, 2012, pp. 161–189, https://doi.org/10.1002/9781118129906.

[26] T.G. Aguirre, C.L. Cramer, V.P. Torres, T.J. Hammann, T.B. Holland, K. Ma, Effects of the addition of boron nitride nanoplate on the fracture toughness, flexural strength, and Weibull Distribution of hydroxyapatite composites prepared by spark plasma sintering, J. Mech. Behav. Biomed. Mater. 93 (2019) 105–117, https://doi.org/10.1016/j.jmbbm.2019.01.021.

[27] B.N. de Souza, M. Dal Bó, D. Hotza, M.C. Fredel, Chemical modification of porcelain tile surface to optimize flexural strength and Weibull modulus through the ion exchange process, J. Build. Eng. 56 (2022) 104735, https://doi.org/10.1016/j.jobe.2022.104735.

[28] D.O. Obada, K.A. Salami, A.A. Alabi, A.N. Oyedeji, S. Csaki, T. Hulan, A.K. Meher, Mechanical behaviour of porous kaolin-based ceramics for potential catalysts support applications, J. Korean Ceram. Soc. 60 (1) (2023) 99–112, https://doi.org/10.1007/s43207-022-00248-3.

[29] A. Winter, A. Schurig, A.L. Odenthal, M. Schmitter, Impact of different layers within a blank on mechanical properties of multi-layered zirconia ceramics before and after thermal ageing, Dent. Mater. 38 (5) (2022) e147–e154, https://doi.org/10.1016/j.dental.2022.03.009.

[30] K. Ono, A simple estimation method of Weibull modulus and verification with strength data, Appl. Sci. 9 (8) (2019) 1575, https://doi.org/10.3390/app9081575.

[31] L. Zerbo, M. Seynou, B. Sorgho, G. Lecomte-Nana, M. Gomina, P. Blanchart, Microstructure and Weibull distribution of rupture strength of clay-talc ceramics, Cerâmica 65 (2019) 240–245, https://doi.org/10.1590/0366-69132019653742518.

[32] A. Buxamusa, *Wind Flow Analysis And Modeling Power Generation For a Multiple Wind Turbine Installation* (Doctoral Dissertation), 2010. http://hdl.handle.net/1989/10652.

[33] M. Rausand, K. Øien, The basic concepts of failure analysis, Reliab. Eng. Syst. Saf. 53 (1) (1996) 73–83, https://doi.org/10.1016/0951-8320(96)00010-5.

[34] L. Xie, Safety Barriers in Complex Systems with Dependent Failures: Modeling and Assessment Approaches, 2022.

[35] C.R. Brooks, A. Choudhury, Failure Analysis of Engineering Materials, McGraw-Hill Education, 2002, https://doi.org/10.1016/j.intermet.2004.04.038.

[36] S.I. Nishida, Failure Analysis in Engineering Applications, Elsevier, 2014.

[37] M. Ortiz, Y. Leroy, A. Needleman, A finite element method for localized failure analysis, Comput. Methods Appl. Mech. Eng. 61 (2) (1987) 189–214, https://doi.org/10.1016/0045-7825(87)90004-1.

[38] T. Liu, Y. Xie, Z. Feng, Y. Luo, K. Wang, W. Xu, A better understanding of the failure modes of tunnels excavated in the boulder-cobble mixed strata by distinct element method, Eng. Fail. Anal. 116 (2020) 104712, https://doi.org/10.1016/j.engfailanal.2020.104712.

[39] Weibull. A Waloddi, Statistical Distribution Function of Wide Applicability, J. Appl. Mech. (1951) 1–6. PP, ffhal-03112318.

[40] T.E. Tay, G. Liu, V.B.C. Tan, X.S. Sun, D.C. Pham, Progressive failure analysis of composites, J. Compos. Mater. 42 (18) (2008) 1921–1966, https://doi.org/10.1177/0021998308093912.

[41] S.S. Scherrer, U. Lohbauer, A. Della Bona, A. Vichi, M.J. Tholey, J.R. Kelly, P.F. Cesar, ADM guidance—ceramics: Guidance to the use of fractography in failure analysis of brittle materials, Dent. Mater. 33 (6) (2017) 599–620, https://doi.org/10.1016/j.dental.2017.03.004.
[42] R.E. Barlow, Engineering Reliability, Society for Industrial and Applied Mathematics, 1998.
[43] R.F. Drenick, Mathematical aspects of the reliability problem, J. Soc. Ind. Appl. Math. 8 (1) (1960) 125–149, https://doi.org/10.1137/0108008.
[44] M. Finkelstein, Failure Rate Modelling for Reliability and Risk, Springer Science & Business Media, 2008.
[45] D.W. Coit, E. Zio, The evolution of system reliability optimization, Reliab. Eng. Syst. Saf. 192 (2019) 106259, https://doi.org/10.1016/j.ress.2018.09.008.
[46] L. Wang, J. Liu, C. Yang, D. Wu, A novel interval dynamic reliability computation approach for the risk evaluation of vibration active control systems based on PID controllers, Appl. Math. Model. 92 (2021) 422–446, https://doi.org/10.1016/j.apm.2020.11.007.
[47] S.M. Aljeddani, M.A. Mohammed, An extensive mathematical approach for wind speed evaluation using inverse Weibull distribution, Alex. Eng. J. 76 (2023) 775–786, https://doi.org/10.1016/j.aej.2023.06.076.
[48] J.E. Breneman, C. Sahay, E.E. Lewis, Introduction to Reliability Engineering, John Wiley & Sons, 2022.
[49] T. Zhu, Reliability estimation for two-parameter Weibull distribution under block censoring, Reliab. Eng. Syst. Saf. 203 (2020) 107071.
[50] S. Acitas, C.H. Aladag, B. Senoglu, A new approach for estimating the parameters of Weibull distribution via particle swarm optimization: an application to the strengths of glass fibre data, Reliab. Eng. Syst. Saf. 183 (2019) 116–127, https://doi.org/10.1016/j.ress.2018.07.024.
[51] E. Xu, F. Zou, P. Shan, A multi-stage fault prediction method of continuous casting machine based on Weibull distribution and deep learning, Alex. Eng. J. 77 (2023) 165–175, https://doi.org/10.1016/j.aej.2023.06.079.
[52] P. Kundu, A.K. Darpe, M.S. Kulkarni, Weibull accelerated failure time regression model for remaining useful life prediction of bearing working under multiple operating conditions, Mech. Syst. Signal Process. 134 (2019) 106302, https://doi.org/10.1016/j.ymssp.2019.106302.
[53] L.A. Pires, L.J. de Azevedo Silva, B.M. Ferrairo, R. Erbereli, J.F.P. Lovo, O.P. Gomes, A.F.S. Borges, Effects of ZnO/TiO2 nanoparticle and TiO2 nanotube additions to dense polycrystalline hydroxyapatite bioceramic from bovine bones, Dent. Mater. 36 (2) (2020) e38–e46, https://doi.org/10.1016/j.dental.2019.11.006.
[54] X. Fan, E.D. Case, I. Gheorghita, M.J. Baumann, Weibull modulus and fracture strength of highly porous hydroxyapatite, J. Mech. Behav. Biomed. Mater. 20 (2013) 283–295, https://doi.org/10.1016/j.jmbbm.2013.01.031.
[55] L. Ćurković, A. Bakić, J. Kodvanj, T. Haramina, Flexural strength of alumina ceramics: Weibull analysis, Trans. FAMENA 34 (1) (2010) 13–18. http://repozitorij.fsb.hr/id/eprint/3589.
[56] H. Yu, J. Li, J. Li, Y. Chen, X. Hou, S. Chen, H. Yang, Biomimetic preparation of a ceramic combined with sea urchin stereo structure and nacre mineral bridge structure, Mater. Des. 178 (2019) 107844, https://doi.org/10.1016/j.matdes.2019.107844.
[57] J.M. Villora, P. Callejas, M.F. Barba, C. Baudın, Statistical analysis of the fracture behaviour of porous ceramic Raschig rings, J. Eur. Ceram. Soc. 24 (3) (2004) 589–594, https://doi.org/10.1016/S0955-2219(03)00245-0.
[58] J.M. Cordell, M.L. Vogl, A.J.W. Johnson, The influence of micropore size on the mechanical properties of bulk hydroxyapatite and hydroxyapatite scaffolds, Journal of the mechanical behaviour of biomedical materials 2 (5) (2009) 560–570, https://doi.org/10.1016/j.jmbbm.2009.01.009.
[59] M.J. Andrews, A.A. Wereszczak, K. Breder, M.K. Ferber, T.P. Kirkland, Investigations of the Weibull modulus as a function of stressing rate, in: 22nd Annual Conference on Composites, Advanced Ceramics, Materials, and Structures: B: Ceramic Engineering and Science Proceedings, John Wiley & Sons, Inc., Hoboken, NJ, USA, 1998, January, pp. 79–87, https://doi.org/10.1002/9780470294499.ch9.
[60] W.S. Lei, Z. Yu, P. Zhang, G. Qian, Standardized Weibull statistics of ceramic strength, Ceram. Int. 47 (4) (2021) 4972–4993, https://doi.org/10.1016/j.ceramint.2020.10.073.
[61] Y.W. Kim, M. Mitomo, N. Hirosaki, R-curve behaviour and microstructure of sintered silicon nitride, J. Mater. Sci. 30 (1995) 5178–5184, https://doi.org/10.1007/BF00356067.
[62] H. Li, Y. Liu, P. Colombo, W. Li, Y. Liu, K. Hu, Z. Lu, The influence of sintering procedure and porosity on the properties of 3D printed alumina ceramic cores, Ceram. Int. 47 (19) (2021) 27668–27676, https://doi.org/10.1016/j.ceramint.2021.06.191.
[63] W. Pabst, T. Uhlířová, Benchmark polynomials for the porosity dependence of elastic moduli and conductivity of partially sintered ceramics, J. Eur. Ceram. Soc. 41 (15) (2021) 7967–7975, https://doi.org/10.1016/j.jeurceramsoc.2021.08.028.
[64] H. Nosrati, R. Sarraf-Mamoory, D.Q.S. Le, R. Zolfaghari Emameh, M. Canillas Perez, C.E. Bünger, Improving the mechanical behaviour of reduced graphene oxide/hydroxyapatite nanocomposites using gas injection into powders synthesis autoclave, Sci. Rep. 10 (1) (2020) 8552, https://doi.org/10.1038/s41598-020-64928-y.
[65] H. Nosrati, R. Sarraf-Mamoory, R. Zolfaghari Emameh, A. Aidun, M. Canillas Perez, Enhancing mechanical properties of hydroxyapatite-reduced graphene oxide nanocomposites by increasing the spark plasma sintering temperature, Inorganic and Nano-Metal Chemistry 51 (11) (2021) 1580–1590, https://doi.org/10.1080/24701556.2020.1852251.
[66] X. Fan, E.D. Case, F. Ren, Y. Shu, M.J. Baumann, Part I: porosity dependence of the Weibull modulus for hydroxyapatite and other brittle materials, J. Mech. Behav. Biomed. Mater. 8 (2012) 21–36, https://doi.org/10.1016/j.jmbbm.2011.12.010.
[67] C.P. Liu, Y.X. Yang, Cytocompatibility evaluation of hydroxyapatite coating on titanium surfaces by pulsed electrochemical deposition, Asian J. Chem. 26 (2014) 5466–5468. WOS:000343769500034.
[68] G.M. Raghavendra, K. Varaprasad, T. Jayaramudu, Biomaterials: design, development and biomedical applications, in: Nanotechnology Applications for Tissue Engineering, William Andrew Publishing, 2015, pp. 21–44, https://doi.org/10.1016/B978-0-323-32889-0.00002-9.
[69] O.A. Osuchukwu, A. Salihi, I. Abdullahi, P.O. Etinosa, D.O. Obada, A comparative study of the mechanical properties of sol-gel derived hydroxyapatite produced from a novel mixture of two natural biowastes for biomedical applications, Mater. Chem. Phys. 297 (2023) 127434, https://doi.org/10.1016/j.matchemphys.2023.127434.
[70] O.A. Osuchukwu, A. Salihi, I. Abdullahi, D.O. Obada, S.A. Abolade, A. Akande, S. Csaki, Structural and nano-mechanical characteristics of a novel mixture of natural hydroxyapatite materials: insights from ab initio calculations and experiments, Mater. Lett. 326 (2022) 132977, https://doi.org/10.1016/j.matlet.2022.132977.
[71] O.A. Osuchukwu, A. Salihi, I. Abdullahi, D.O. Obada, Taguchi grey relational optimization of sol–gel derived hydroxyapatite from a novel mix of two natural biowastes for biomedical applications, Sci. Rep. 12 (1) (2022) 17968, https://doi.org/10.1038/s41598-022-22888-5.
[72] O.A. Osuchukwu, A. Salihi, I. Abdullahi, D.O. Obada, S.A. Abolade, A. Akande, D. Dodoo-Arhin, Datasets on the elastic and mechanical properties of hydroxyapatite: a first principle investigation, experiments, and pedagogical perspective, Data Brief 48 (2023) 109075, https://doi.org/10.1016/j.dib.2023.109075.
[73] O.A. Osuchukwu, A. Salihi, I. Abdullahi, D.O. Obada, Experimental data on the characterization of hydroxyapatite produced from a novel mixture of biowastes, Data Brief 42 (2022) 108305, https://doi.org/10.1016/j.dib.2022.108305.
[74] O.A. Osuchukwu, A. Salihi, I. Abdullahi, B. Abdulkareem, C.S. Nwannenna, Synthesis techniques, characterization and mechanical properties of naturally derived hydroxyapatite scaffolds for bone implants: a review, SN Appl. Sci. 3 (2021) 1–23, https://doi.org/10.1007/s42452-021-04795-y.
[75] C.E. Seow, J. Zhang, H.E. Coules, G. Wu, C. Jones, J. Ding, S. Williams, Effect of crack-like defects on the fracture behaviour of Wire+ arc additively manufactured nickel-base alloy 718, Addit. Manuf. 36 (2020) 101578, https://doi.org/10.1016/j.addma.2020.101578.
[76] Z. Guan, H. Tian, N. Li, J. Long, W. Zhang, Y. Du, High-accuracy reliability evaluation for the WC–Co-based cemented carbides assisted by machine learning, Ceram. Int. 49 (1) (2023) 613–624, https://doi.org/10.1016/j.ceramint.2022.09.030.
[77] Y. Tanaka, H. Sato, O. Eryu, Improved cemented carbide tool edge formed by solid phase chemical–mechanical polishing, J. Mater. Res. Technol. 20 (2022) 606–615, https://doi.org/10.1016/j.jmrt.2022.07.077.
[78] X.K. Li, S.P. Zhu, D. Liao, J.A. Correia, F. Berto, Q. Wang, Probabilistic fatigue modelling of metallic materials under notch and size effect using the weakest link theory, Int. J. Fatig. 159 (2022) 106788, https://doi.org/10.1016/j.ijfatigue.2022.106788.
[79] T. Klünsner, S. Wurster, P. Supancic, R. Ebner, M. Jenko, J. Glätzle, R. Pippan, Effect of specimen size on the tensile strength of WC–Co hard metal, Acta Mater. 59 (10) (2011) 4244–4252, https://doi.org/10.1016/j.actamat.2011.03.049.

[80] J.M. Tarragó, D. Coureaux, Y. Torres, E. Jiménez-Piqué, L. Schneider, J. Fair, L. Llanes, Strength and reliability of WC-Co cemented carbides: understanding microstructural effects based on R-curve behaviour and fractography, Int. J. Refract. Metals Hard Mater. 71 (2018) 221–226, https://doi.org/10.1016/j.ijrmhm.2017.11.031.

[81] H. Tian, J. Chen, G. Zhu, Y. Du, Y. Peng, Investigation of WC–Co alloy properties based on thermodynamic calculation and Weibull distribution, Mater. Sci. Technol. 35 (18) (2019) 2269–2274, https://doi.org/10.1080/02670836.2019.1671645.

[82] O.A. Osuchukwu, A. Salihi, I. Abdullahi, P.O. Etinosa, D.O. Obada, Weibull modulus of a novel mixture of natural hydroxyapatite materials produced from biowastes, Results in Materials 18 (2023) 100394, https://doi.org/10.1016/j.rinma.2023.100394.

[83] R. Danzer, A general strength distribution function for brittle materials, J. Eur. Ceram. Soc. 10 (6) (1992) 461–472, https://doi.org/10.1016/0955-2219(92)90021-5.

[84] D.L. Nguyen, D.K. Thai, T.T. Ngo, T.K. Tran, T.T. Nguyen, Weibull modulus from size effect of high-performance fibre-reinforced concrete under compression and flexure, Construct. Build. Mater. 226 (2019) 743–758, https://doi.org/10.1016/j.conbuildmat.2019.07.234.

[85] J.M. Tarragó, D. Coureaux, Y. Torres, D. Casellas, I. Al-Dawery, L. Schneider, L. Llanes, Microstructural effects on the R-curve behaviour of WC-Co cemented carbides, Mater. Des. 97 (2016) 492–501, https://doi.org/10.1016/j.matdes.2016.02.115.

[86] D.L. Nguyen, H.V. Le, V.T. Nguyen, N.T. Tran, Evaluating fracture characteristics of ultra-high-performance fibre-reinforced concrete in flexure and tension with size impact, Construct. Build. Mater. 382 (2023) 131224, https://doi.org/10.1016/j.conbuildmat.2023.131224.

[87] C. Zhang, Z. Wu, C. Luo, X. Hu, K. Li, C. Shi, N. Banthia, Size effect of ultra-high-performance concrete under compression: effects of steel fibre characteristics and water-to-binder ratio, Construct. Build. Mater. 330 (2022) 127170, https://doi.org/10.1016/j.conbuildmat.2022.127170.

[88] S.J. Al-Malki, Statistical Analysis of Lifetime Data Using Newly Modified Weibull Distributions, The University of Manchester, United Kingdom, 2014.

[89] Jr A.J. Hallinan, A review of the Weibull distribution, J. Qual. Technol. 25 (2) (1993) 85–93, https://doi.org/10.1080/00224065.1993.11979431.

[90] H. Teimourian, M. Abubakar, M. Yildiz, A. Teimourian, A comparative study on wind energy assessment distribution models: a case study on Weibull distribution, Energies 15 (15) (2022) 5684, https://doi.org/10.3390/en15155684.

[91] M.A. Alomair, Z. Ahmad, G.S. Rao, H. Al-Mofleh, S.K. Khosa, A.S. Al Naim, A new trigonometric modification of the Weibull distribution: control chart and applications in quality control, PLoS One 18 (7) (2023) e0286593, https://doi.org/10.1371/journal.pone.0286593.

[92] C. Shi, H. Yu, G. Qian, X. Li, X. Zhu, D. Yao, C. Zhang, Research on the characteristics of asphalt mixture gradation curve based on Weibull distribution, Construct. Build. Mater. 366 (2023) 130151, https://doi.org/10.1016/j.conbuildmat.2022.130151.

[93] C. Sinner, Y. Dominicy, J. Trufin, W. Waterschoot, P. Weber, C. Ley, From pareto to weibull–A constructive review of distributions on $\mathbb{R}+$, Int. Stat. Rev. 91 (1) (2023) 35–54, https://doi.org/10.1111/insr.12508.

[94] H. Yin, X. He, G. Song, Y. Zheng, Y. Bai, Statistical analysis of the strength reliability of the MAX phases, J. Am. Ceram. Soc. 106 (2) (2023) 1321–1332, https://doi.org/10.1111/jace.18829.

[95] A. Boulebnane, D. Djeghader, T. Tioua, Weibull analysis of charpy impact test in short date palm fiber reinforced epoxy composite, Period. Polytech. Civ. Eng. (2023), https://doi.org/10.3311/PPci.22500.

[96] W. Weibull, A Statistical Theory of Strength of Materials. *IVB-Handl*, 1939.

[97] 4. Pierce, Tensile tests for cotton yarns. v.-'the weakest link', theorems on the strength of long composite specimens, J. Textile Inst 17 (1926) T355–T368.

[98] P.K. Suri, P. Raheja, A study on Weibull distribution for estimating the reliability, International Journal of Engineering and Computer Science 4 (7) (2015).

[99] A. Dey, A.K. Mukhopadhyay, S. Gangadharan, M.K. Sinha, D. Basu, Weibull modulus of nano-hardness and elastic modulus of hydroxyapatite coating, J. Mater. Sci. 44 (2009) 4911–4918, https://doi.org/10.1007/s10853-009-3750-y.

[100] J. Campbell, M. Tiryakioğlu, Bifilm defects in Ni-based alloy castings, Metall. Mater. Trans. B 43 (2012) 902–914, https://doi.org/10.1007/s11663-011-9577-3.

[101] M. Tiryakioğlu, D. Hudak, Guidelines for two-parameter Weibull analysis for flaw-containing materials, Metall. Mater. Trans. B 42 (2011) 1130–1135, https://doi.org/10.1007/s11663-011-9556-8.

[102] G. Mueller, S.E. Rigdon, The constant shape parameter assumption in Weibull regression, Qual. Eng. 27 (3) (2015) 374–392, https://doi.org/10.1080/08982112.2015.1041607.

[103] M. Maswadah, Improved maximum likelihood estimation of the shape-scale family based on the generalized progressive hybrid censoring scheme, J. Appl. Stat. 49 (11) (2022) 2825–2844, https://doi.org/10.1080/02664763.2021.1924638.

[104] D. Galar, U. Kumar, Chapter 6-prognosis, EMaintenance (2017) 311–370, https://doi.org/10.1016/B978-0-12-811153-6.00006-3.

[105] M.G. Khan, M.R. Ahmed, Bayesian method for estimating Weibull parameters for wind resource assessment in the tropical region: a comparison between two-parameter and three-parameter Weibull distributions, Wind Energy Science 8 (8) (2023) 1277–1298. http://repository.usp.ac.fj/id/eprint/14154.

[106] A. Gupta, M. Singh, J.S. Saini, Effect of nano-silica on fatigue behaviour of glass fiber-reinforced epoxy composite laminates: a Weibull distribution approach, Polym. Compos. (2023), https://doi.org/10.1002/pc.27761.

[107] H.S. Bakouch, Using the Weibull Distribution: Reliability, Modelling and Inference, 2014.

[108] D.P. Murthy, M. Xie, R. Jiang, Weibull Models, John Wiley & Sons, 2004.

[109] R. Belli, U. Lohbauer, The breakdown of the Weibull behaviour in dental zirconias, J. Am. Ceram. Soc. 104 (9) (2021) 4819–4828, https://doi.org/10.1111/jace.17886.

[110] H. Mano, T. Ohana, Evaluation of anti-adhesion characteristics of diamond-like carbon film by combining friction and wear test with step loading and Weibull analysis, Materials 14 (11) (2021) 2746, https://doi.org/10.3390/ma14112746.

[111] J.I. McCool, Using the Weibull Distribution: Reliability, Modelling, and Inference, vol. 950, John Wiley & Sons, 2012.

[112] C. Liu, R.W. White, S. Dumais, Understanding web browsing behaviours through Weibull analysis of dwell time, in: Proceedings of the 33rd International ACM SIGIR Conference on Research and Development in Information Retrieval, 2010, July, pp. 379–386, https://doi.org/10.1145/1835449.1835513.

[113] P. Bhattacharya, R. Bhattacharjee, A study on Weibull distribution for estimating the parameters, Journal of Applied Quantitative Methods 5 (2) (2010) 234–241.

[114] Y.M. Kantar, B. Şenoğlu, A comparative study for the location and scale parameters of the Weibull distribution with given shape parameters, Comput. Geosci. 34 (12) (2008) 1900–1909, https://doi.org/10.1016/j.cageo.2008.04.004.

[115] J. Kohout, Four-parameter Weibull distribution with lower and upper limits applicable in reliability studies and materials testing, Mathematics 11 (3) (2023) 544, https://doi.org/10.3390/math11030544.

[116] M. Bebbington, C.D. Lai, M. Wellington, R. Zitikis, The discrete additive Weibull distribution: a bathtub-shaped hazard for discontinuous failure data, Reliab. Eng. Syst. Saf. 106 (2012) 37–44, https://doi.org/10.1016/j.ress.2012.06.009.

[117] M. Tiryakioğlu, J. Campbell, Weibull analysis of mechanical data for castings: a guide to the interpretation of probability plots, Metall. Mater. Trans. 41 (2010) 3121–3129, https://doi.org/10.1007/s11661-010-0364-6.

[118] Y.K. Chu, J.C. Ke, Computation approaches for parameter estimation of Weibull distribution, Math. Comput. Appl. 17 (1) (2012) 39–47, https://doi.org/10.3390/mca17010039.

[119] E.M. Almetwally, H.M. Almongy, Estimation methods for the new weibull-pareto distribution: simulation and application, J. Data Sci. 17 (3) (2019) 610–630, https://doi.org/10.6339/JDS.201906_17(3).0009.

[120] S. Jiang, D. Kececioglu, Graphical representation of two mixed-Weibull distributions, IEEE Trans. Reliab. 41 (2) (1992) 241–247, https://doi.org/10.1109/24.257791.

[121] N. Feroze, M. Aslam, T.N. Sindhu, M. Noor-ul-Amin, Mixed Weibull distributions for the Bayesian analysis of reliability when failures are progressively censored, J. Stat. Comput. Simulat. 91 (17) (2021) 3505–3529, https://doi.org/10.1080/00949655.2021.1942470.

[122] X. Dong, R. Zheng, A graphical method-genetic algorithm (GMGA) approach for parameter estimation of twofold Weibull mixture model, in: 2020 7th International Conference on Information Science and Control Engineering (ICISCE), IEEE, 2020, December, pp. 8–12, https://doi.org/10.1109/ICISCE50968.2020.00012.

[123] D. Kundu, M.Z. Raqab, Generalized Rayleigh distribution: different methods of estimations, Comput. Stat. Data Anal. 49 (1) (2005) 187–200, https://doi.org/10.1016/j.csda.2004.05.008.
[124] Y. Ai, S.P. Zhu, D. Liao, J.A.F.O. Correia, C. Souto, A.M.P. De Jesus, B. Keshtegar, Probabilistic modelling of fatigue life distribution and size effect of components with random defects, Int. J. Fatig. 126 (2019) 165–173, https://doi.org/10.1016/j.ijfatigue.2019.05.005.
[125] J. Lienig, H. Bruemmer, Fundamentals of Electronic Systems Design, Springer International Publishing, Cham, 2017, p. 54.
[126] H. Zhou, M. Farsi, A. Harrison, A.K. Parlikad, A. Brintrup, Civil aircraft engine operation life resilient monitoring via usage trajectory mapping on the reliability contour, Reliab. Eng. Syst. Saf. 230 (2023) 108878, https://doi.org/10.1016/j.ress.2022.108878.
[127] R. Jiang, A new bathtub curve model with a finite support, Reliab. Eng. Syst. Saf. 119 (2013) 44–51, https://doi.org/10.1016/j.ress.2013.05.019.
[128] X.C. Li, M. Meng, D. Li, R. Wei, L. He, S.F. Zhang, Strengthening and toughening of a multi-component lithium disilicate glass-ceramic by ion exchange, J. Eur. Ceram. Soc. 40 (13) (2020) 4635–4646, https://doi.org/10.1016/j.jeurceramsoc.2020.05.075.
[129] J.W. Evans, D.E. Kretschmann, D.W. Green, Procedures for Estimation of Weibull Parameters, United States Department of Agriculture, Forest Service, 2019, p. 17. Forest Products Laboratory.
[130] P. Bhattacharya, R. Bhattacharjee, A study on Weibull distribution for estimating the parameters, Journal of Applied Quantitative Methods 5 (2) (2010) 234–241.
[131] M. Sumair, T. Aized, S.A.R. Gardezi, S.U. ur Rehman, S.M.S. Rehman, A novel method was developed to estimate Weibull parameters, Energy Rep. 6 (2020) 1715–1733, https://doi.org/10.1016/j.egyr.2020.06.017.
[132] M.G.M. Khan, M.R. Ahmed, Bayesian method for estimating Weibull parameters for wind resource assessment in the Equatorial region: a comparison between two-parameter and three-parameter Weibull distributions, Wind Energy Science Discussions 2022 (2022) 1–38, https://doi.org/10.5194/wes-8-1277-2023.
[133] B. Dodson, The Weibull Analysis Handbook, 2006.
[134] ASTM Committee C-28 on Advanced Ceramics, Standard Practice for Reporting Uniaxial Strength Data and Estimating Weibull Distribution Parameters for Advanced Ceramics, ASTM international, 2007.
[135] J. Gong, A new probability index for estimating Weibull modulus for ceramics with the least-square method, J. Mater. Sci. Lett. 19 (10) (2000) 827–829, https://doi.org/10.1023/A:1006712809728.
[136] L. Song, D. Wu, Y. Li, Optimal probability estimators for determining Weibull parameters, J. Mater. Sci. Lett. 22 (23) (2003) 1651–1653, https://doi.org/10.1023/B:JMSL.0000004640.71595.f3.
[137] X. Yang, L. Xie, J. Song, J. Chen, B. Zhao, Y. Yang, Effect analysis of probability estimators on parameter estimation of the three-parameter Weibull distribution, Int. J. Struct. Stabil. Dynam. (2023) 2450009, https://doi.org/10.1142/S0219455424500093.
[138] X. Liu, N. Xie, Grey-based approach for estimating the Weibull model and its application, Commun. Stat. Theor. Methods 52 (21) (2023) 7601–7617, https://doi.org/10.1080/03610926.2022.2050397.
[139] G. Blom, Statistical Estimates and Transformed Beta-Variables (Doctoral Dissertation, Almqvist & Wiksell), 1958.
[140] E. Mackay, P. Jonathan, Sampling properties and empirical estimates of extreme events, Ocean Engineering 239 (2021) 109791, https://doi.org/10.1016/j.oceaneng.2021.109791.
[141] D. Koutsoyiannis, Knowable moments in stochastics: knowing their advantages, Axioms 12 (6) (2023) 590, https://doi.org/10.3390/axioms12060590.
[142] R. Gnanadesikan, M.B. Wilk, Probability plotting methods for the analysis of data, Biometrika 55 (1) (1968) 1–17, https://doi.org/10.1093/biomet/55.1.1.
[143] D. Luo, W. Cheng, D. Xu, W. Yu, B. Zong, H. Chen, X. Zhang, Parameterized explainer for graph neural network, Adv. Neural Inf. Process. Syst. 33 (2020) 19620–19631.
[144] H. Yuan, J. Tang, X. Hu, S. Ji, Xgnn: towards model-level explanations of graph neural networks, in: Proceedings of the 26th ACM SIGKDD International Conference on Knowledge Discovery & Data Mining, 2020, August, pp. 430–438, https://doi.org/10.1145/3394486.3403085.
[145] A. Saghafi, A.R. Mirhabibi, G.H. Yari, Improved linear regression method for estimating Weibull parameters, Theor. Appl. Fract. Mech. 52 (3) (2009) 180–182, https://doi.org/10.1016/j.tafmec.2009.09.007.
[146] B. Deng, D. Jiang, Determination of the Weibull parameters from the mean value and the coefficient of variation of the measured strength for brittle ceramics, Journal of Advanced Ceramics 6 (2017) 149–156, https://doi.org/10.1007/s40145-017-0227-3.
[147] M.A. Madjoubi, C. Bousbaa, M. Hamidouche, N. Bouaouadja, Weibull statistical analysis of the mechanical strength of a glass eroded by sandblasting, J. Eur. Ceram. Soc. 19 (16) (1999) 2957–2962, https://doi.org/10.1016/S0955-2219(99)00087-4.
[148] R. Danzer, Some notes on the correlation between fracture and defect statistics: are Weibull statistics valid for very small specimens? J. Eur. Ceram. Soc. 26 (15) (2006) 3043–3049, https://doi.org/10.1016/j.jeurceramsoc.2005.08.021.
[149] C. Qi, C. Lu, A.I. Chanyshev, X. Li, X. Qu, Preliminary Study on the Determination of the Weibull modulus of strength distribution in quasi-brittle materials, Geohazard Mechanics (2023), https://doi.org/10.1016/j.ghm.2023.05.002.
[150] A.Z.A. Ani, S.A. Zaidan, Determine Weibull modulus in terms of electrical strength and piston-on-three-balls test to characterize polyester-nano silica composites, in: AIP Conference Proceedings, vol. 2475, AIP Publishing, 2023, March, https://doi.org/10.1063/5.0104684, 1.
[151] P.L. Bonate, A brief introduction to Monte Carlo simulation, Clin. Pharmacokinet. 40 (2001) 15–22, https://doi.org/10.2165/00003088-200140010-00002.
[152] J.A. Purton, J.C. Crabtree, S.C. Parker, DL_MONTE: a general-purpose program for parallel Monte Carlo simulation, Mol. Simulat. 39 (14–15) (2013) 1240–1252, https://doi.org/10.1080/08927022.2013.839871.
[153] M. Fippel, A.G. Brainlab, Basics of Monte Carlo simulations, in: Monte Carlo Techniques in Radiation Therapy, CRC Press, 2021, pp. 17–28.
[154] K. Binder, Monte Carlo simulations in statistical physics, in: Statistical and Nonlinear Physics, Springer US, New York, NY, 2022, pp. 85–97, https://doi.org/10.1007/978-3-642-27737-5_337-2.
[155] R.B. Malidarre, F. Kulali, A. Inal, A. Oz, Monte Carlo simulation of a waste soda–lime–silica glass system containing Sb2O3 for gamma-ray shielding, Emerg. Mater. Res. 9 (4) (2020) 1334–1340, https://doi.org/10.1680/jemmr.20.00202.
[156] W. Li, Reliability Assessment of Electric Power Systems Using Monte Carlo Methods, Springer Science & Business Media, 2013.
[157] S. Mahadevan, Monte Carlo simulation, Mechanical Engineering-New York and Basel-Marcel Dekker- (1997) 123–146.
[158] D.K. Lee, J. In, S. Lee, Standard deviation and standard error of the mean, Korean Journal of Anesthesiology 68 (3) (2015) 220–223, https://doi.org/10.4097/kjae.2015.68.3.220.
[159] M. Kelly, The Standard Errors of Persistence, 2019.
[160] D. Vats, K. Gupta, An Introduction to Estimating Monte Carlo Standard Errors with R Package Mcmcse, 2021.
[161] B. Jann, Influence Functions Continued. A Framework for Estimating Standard Errors in Reweighting, Matching, and Regression Adjustment, 2020.
[162] P. Cummings, Adjusting standard errors and confidence intervals, in: Analysis of Incidence Rates, Chapman and Hall/CRC, 2019, pp. 233–248, 9780429055713.
[163] W. Chen, P. Hribar, S. Melessa, Standard error biases when using generated regressors in accounting research, J. Account. Res. 61 (2) (2023) 531–569.
[164] X. Hu, G. Fang, J. Yang, L. Zhao, Y. Ge, Simplified models for uncertainty quantification of extreme events using the Monte Carlo technique, Reliab. Eng. Syst. Saf. 230 (2023) 108935, https://doi.org/10.1016/j.ress.2022.108935.
[165] T. Schamberger, Conducting Monte Carlo simulations with PLS-PM and other variance-based estimators for structural equation models: a tutorial using the R package cSEM, Ind. Manag. Data Syst. 123 (6) (2023) 1789–1813, https://doi.org/10.1108/IMDS-07-2022-0418.
[166] D. Karunarasan, R. Sooriyarachchi, V. Pinto, A comparison of Bayesian Markov chain Monte Carlo methods in a multilevel scenario, Commun. Stat. Simulat. Comput. 52 (10) (2023) 4756–4772, https://doi.org/10.1080/03610918.2021.1967985.
[167] Y. Yao, X. Wang, X. Chen, J. Yu, S. Liu, Novel diversity/MIMO PIFA antenna with broadband circular polarization for multimode satellite navigation, IEEE Antenn. Wireless Propag. Lett. 11 (2012) 65–68.
[168] P. Paul, M.L. Pennell, S. Lemeshow, Standardizing the power of the Hosmer–Lemeshow goodness of fit test in large data sets, Stat. Med. 32 (1) (2013) 67–80, https://doi.org/10.1002/sim.5525.

[169] M. Aslam, A new goodness of fit test in the presence of uncertain parameters, Complex & Intelligent Systems 7 (1) (2021) 359–365, https://doi.org/10.1007/s40747-020-00214-8.
[170] S.O. Susam, B. Hudaverdi Ucer, A goodness-of-fit test based on Bézier curve estimation of Kendall distribution, J. Stat. Comput. Simulat. 90 (7) (2020) 1194–1215, https://doi.org/10.1080/00949655.2020.1720680.
[171] M.H. Pham, C. Tsokos, B.J. Choi, Maximum likelihood estimation for the generalized Pareto distribution and goodness-of-fit test with censored data, J. Mod. Appl. Stat. Methods 17 (2) (2019) 11, https://doi.org/10.22237/jmasm/1553261471.
[172] online].Available:https://www.ge.com/digital/documentation/meridium/V36160/Help/Master/Subsystems/Reliability/Content/Goodness_of_Fit_(GOF)_Tests_for_a_Weibull_Distribution.htm.
[173] C. Park, Weibullness test and parameter estimation of the three-parameter Weibull model using the sample correlation coefficient, International Journal of Industrial Engineering: Theory, Applications and Practice 24 (4) (2017) 376–391.
[174] C. Park, X. Gao, M. Wang, Robust explicit estimators using the power-weighted repeated medians, J. Appl. Stat. (2023) 1–19, https://doi.org/10.1080/02664763.2023.2229969.
[175] X. Yang, L. Xie, B. Zhao, X. Kong, N. Wu, An iterative method for parameter estimation of the three-parameter Weibull distribution based on a small sample size with a fixed shape parameter, Int. J. Struct. Stabil. Dynam. 22 (12) (2022) 2250125.
[176] C. Park, A note on the existence of the location parameter estimate of the three-parameter Weibull model using the Weibull plot, Math. Probl Eng. 2018 (2018).
[177] G.P. Patil, S. Kotz, J.K. Ord (Eds.), A Modern Course on Statistical Distributions in Scientific Work: Proceedings of the NATO Advanced Study Institute Held at the University of Calgary, vol. 17, Springer Science & Business Media, Calgary, Alberta, 2012. Canada July 29–August 10, 1974.
[178] M. Tiryakioğlu, D. Hudak, G. Ökten, On evaluating Weibull fits to mechanical testing data, Materials Science and Engineering: A 527 (1–2) (2009) 397–399, https://doi.org/10.1016/j.msea.2009.08.014.
[179] N.R. Green, J. Campbell, Influence of oxide film filling defects on the strength of Al-7Si-Mg alloy castings (94-114), Trans. Am. Foundrymen's Soc. 102 (1994) 341–348.
[180] N.R. Green, J. Campbell, Statistical distributions of fracture strengths of cast Al 7Si Mg alloy, Materials Science and Engineering: A 173 (1–2) (1993) 261–266, https://doi.org/10.1016/0921-5093(93)90226-5.
[181] M. Tiryakioğlu, D. Hudak, Unbiased estimates of the Weibull parameters by the linear regression method, J. Mater. Sci. 43 (2008) 1914–1919, https://doi.org/10.1007/s10853-008-2457-9.
[182] United States. Dept. of Defense, Military Handbook: Metallic Materials and Elements for Aerospace Vehicle Structures, vol. 1, US Department of Defense, 1990.
[183] Y. Wang, W. Yu, F. Wang, Experimental evaluation and modified Weibull characterization of the tensile behaviour of tri-component elastic-conductive composite yarn, Textil. Res. J. 88 (10) (2018) 1138–1149.
[184] J.C. Fothergill, Estimating the cumulative probability of failure data points to be plotted on Weibull and other probability papers, IEEE Trans. Electr. Insul. 25 (3) (1990) 489–492, https://doi.org/10.1109/14.55721.
[185] G. Nilakantan, A.A. Obaid, M. Keefe, J.W. Gillespie Jr, Experimental evaluation and statistical characterization of the strength and strain energy density distribution of Kevlar KM2 yarns: exploring length-scale and weaving effects, J. Compos. Mater. 45 (17) (2011) 1749–1769.
[186] M. Nassar, A.Z. Afify, M.K. Shakhatreh, S. Dey, On a new extension of Weibull distribution: properties, estimation, and applications to one and two causes of failures, Qual. Reliab. Eng. Int. 36 (6) (2020) 2019–2043, https://doi.org/10.1002/qre.2671.
[187] P. Strzelecki, Determination of fatigue life for low probability of failure for different stress levels using 3-parameter Weibull distribution, Int. J. Fatig. 145 (2021) 106080, https://doi.org/10.1016/j.ijfatigue.2020.106080.
[188] D. Djeghader, B. Redjel, Weibull analysis of fatigue test in jute-reinforced polyester composite material, Compos. Commun. 17 (2020) 123–128, https://doi.org/10.1016/j.coco.2019.11.016.
[189] G.A. Bohoris, Gamma function tables for the estimation of the mean and standard deviation of the Weibull distribution, Qual. Reliab. Eng. Int. 10 (2) (1994) 105–115, https://doi.org/10.1002/qre.4680100205.
[190] G. Zhou, G.A.O. Davies, Characterization of thick glass woven roving/polyester laminates: 2. Flexure and statistical considerations, Composites 26 (8) (1995) 587–596, https://doi.org/10.1016/0010-4361(95)92623-K.
[191] M.E. Mead, A. Afify, N.S. Butt, The Modified Kumaraswamy Weibull Distribution: Properties and Applications in Reliability and Engineering Sciences, Pakistan Journal of Statistics and Operation Research, 2020, pp. 433–446, https://doi.org/10.18187/pjsor.v16i3.3306.
[192] E.K. Babacan, K.A.Y.A. Samet, Comparison of parameter estimation methods in Weibull Distribution, Sigma J. Eng. Nat. Sci. 38 (3) (2020) 1609–1621.
[193] B.P. Revol, M. Thomassey, F. Ruch, M. Nardin, Influence of the sample number for the prediction of the tensile strength of high-tenacity viscose fibres using a two-parameter Weibull distribution, Cellulose 23 (4) (2016) 2701–2713, https://doi.org/10.1007/s10570-016-0974-2.
[194] B. Sürücü, H.S. Sazak, Monitoring reliability for a three-parameter Weibull distribution, Reliab. Eng. Syst. Saf. 94 (2) (2009) 503–508, https://doi.org/10.1016/j.ress.2008.06.001.
[195] Y. Wang, Z. Chen, Y. Zhang, X. Li, Z. Li, Remaining useful life prediction of rolling bearings based on the three-parameter Weibull distribution proportional hazards model, Insight-Non-Destructive Testing and Condition Monitoring 62 (12) (2020) 710–718, https://doi.org/10.1784/insi.2020.62.12.710.
[196] G.H. Reddy, A.N. Koundinya, S. Gope, C. Behera, Lifetime estimation of electrical equipment in distribution system using modified 3-parameter Weibull distribution, in: 2021 International Conference on Design Innovations for 3Cs Compute Communicate Control (ICDI3C), IEEE, 2021, June, pp. 21–26, https://doi.org/10.1109/ICDI3C53598.2021.00013.
[197] D. Kececioglu, Reliability Engineering Handbook, vol. 1, DEStech Publications, Inc, 2002.
[198] T. Bučar, M. Nagode, M. Fajdiga, Reliability approximation using finite Weibull mixture distributions, Reliab. Eng. Syst. Saf. 84 (3) (2004) 241–251, https://doi.org/10.1016/j.ress.2003.11.008.
[199] E. Jahanbani, A.T.P. Najafabadi, K. Masoumifard, On Bayesian credibility mean for finite mixture distributions, Ann. Actuar. Sci. (2023) 1–25, https://doi.org/10.1017/S1748499523000076.
[200] S. Zacks, Introduction to Reliability Analysis: Probability Models and Statistical Methods, Springer Science & Business Media, 2012.
[201] L.M. Leemis, Reliability: Probabilistic Models and Statistical Methods, Prentice-Hall, Inc., 1995.
[202] D.F. Falaakh, P. Myers, J.P. Park, G.S. Was, C.B. Bahn, Statistical determination of stress threshold and survival analysis on IASCC initiation data of stainless steels in pressurized water reactor conditions, J. Nucl. Mater. 154549 (2023), https://doi.org/10.1016/j.jnucmat.2023.154549.
[203] R. Jiang, D.N.P. Murthy, P. Ji, Models involving two inverse Weibull distributions, Reliab. Eng. Syst. Saf. 73 (1) (2001) 73–81, https://doi.org/10.1016/S0951-8320(01)00030-8.
[204] R. Jiang, D.N.P. Murthy, P. Ji, n-fold Weibull multiplicative model, Reliab. Eng. Syst. Saf. 74 (2) (2001) 211–219, https://doi.org/10.1016/S0951-8320(01)00108-9.
[205] R. Jiang, F. Qi, Y. Cao, Relation between ageing intensity function and WPP plot and its application in reliability modelling, Reliab. Eng. Syst. Saf. 229 (2023) 108894, https://doi.org/10.1016/j.ress.2022.108894.
[206] M.F. Ramalhoto, M. Morais, Shewhart control charts for the scale parameter of a Weibull control variable with fixed and variable sampling intervals, J. Appl. Stat. 26 (1) (1999) 129–160, https://doi.org/10.1080/02664769922700.
[207] R.M. Vasconcelos, R.C. Quinino, L.L. Ho, F.R. Cruz, About Shewhart control charts to monitor the Weibull mean based on a Gamma distribution, Qual. Reliab. Eng. Int. 38 (8) (2022) 4210–4222, https://doi.org/10.1002/qre.3200.
[208] D. Yu, L. Jin, J. Li, X. Qin, Z. Zhu, J. Zhang, Monitoring the Weibull scale parameter based on type I censored data using a modified EWMA control chart, Axioms 12 (5) (2023) 487, https://doi.org/10.3390/axioms12050487.
[209] M.F. Zambak, The probability density function for wind speed using modified Weibull distribution, Int. J. Energy Econ. Pol. 11 (6) (2021) 544–550.
[210] R. Luus, M. Jamme, Estimation of parameters in 3-parameter Weibull probability distribution functions, Hungar. J. Ind. Chem. 33 (1–2) (2005).
[211] M.Q. Islam, M.L. Tiku, F. Yildirim, Nonnormal regression. I. Skew distributions, Commun. Stat. Theor. Methods 30 (6) (2001) 993–1020, https://doi.org/10.1081/STA-100104347.

[212] Y. Zhang, Y. Liu, S. Xu, Arbitrary-order Taylor series expansion-based viscoacoustic wavefield simulation in 3D vertical transversely isotropic media, Geophys. Prospect. 68 (8) (2020) 2379–2399, https://doi.org/10.1111/1365-2478.12999.
[213] A.M. Basheer, Alpha power inverse Weibull distribution with reliability application, J. Taibah Univ. Sci. 13 (1) (2019) 423–432, https://doi.org/10.1080/16583655.2019.1588488.
[214] M. Li, X. Liu, Maximum likelihood least squares-based iterative estimation for a class of bilinear systems using the data filtering technique, Int. J. Control Autom. Syst. 18 (6) (2020) 1581–1592, https://doi.org/10.1007/s12555-019-0191-5.
[215] T. Arslan, S. Acitas, B. Senoglu, Modified minimum distance estimators: definition, properties and applications, Comput. Stat. 37 (4) (2022) 1551–1568, https://doi.org/10.1007/s00180-021-01170-8.
[216] J.P. Nolan, Univariate Stable Distributions, Springer International Publishing, Cham, 2020.
[217] A. Maydeu-Olivares, D. Shi, Y. Rosseel, Instrumental variables two-stage least squares (2SLS) vs. maximum likelihood structural equation modelling of causal effects in linear regression models, Struct. Equ. Model.: A Multidiscip. J. 26 (6) (2019) 876–892, https://doi.org/10.1080/10705511.2019.1607740.
[218] O.J.E. Ouédraogo, E. Katchekpele, S. Dossou-Gbété, Marginalized maximum likelihood for parameters estimation of the three parameter Weibull distribution, Int. J. Stat. Probab. 10 (4) (2021).
[219] N. Taketomi, K. Yamamoto, C. Chesneau, T. Emura, Parametric distributions for survival and reliability analyses, a review and historical sketch, Mathematics 10 (20) (2022) 3907, https://doi.org/10.3390/math10203907.
[220] A.K. Srivastava, Bayesian approach in estimation of shape and scale parameter of log-weibull model, International Journal of Innovative Science, Engineering & Technology 6 (12) (2019) 185–196.
[221] M. Alslman, A. Helu, Estimation of the stress-strength reliability for the inverse Weibull distribution under adaptive type-II progressive hybrid censoring, PLoS One 17 (11) (2022) e0277514, https://doi.org/10.1371/journal.pone.0277514.
[222] W.B. Nelson, Applied Life Data Analysis, John Wiley & Sons, 2005.
[223] Y. Gao, X. Huang, J. Wu, Q. Zhou, An order statistic approach for inference of the size distribution of 3D particle clusters in metal matrix nanocomposites, CIRP Journal of Manufacturing Science and Technology 38 (2022) 204–214, https://doi.org/10.1016/j.cirpj.2022.04.015.
[224] J. NL Johnson Antoch, S. Kotz, N. Balakrishnan, Continuous Univariate Distributions, vol. 1, John Wiley, New York, 1994 xix+ 756, Price: g 66.00, ISBN 0-471-58495-9.
[225] W.Q. Meeker, L.A. Escobar, F.G. Pascual, Statistical Methods for Reliability Data, John Wiley & Sons, 2022.
[226] J.F. Lawless, Statistical Models and Methods for Lifetime Data, John Wiley & Sons, 2011.
[227] D. Gaspar, L.A. Ferreira, A simulation of data censored rigth type I with Weibull distribution, in: 2022 6th International Conference on System Reliability and Safety (ICSRS), IEEE, 2022, November, pp. 505–511, https://doi.org/10.1109/ICSRS56243.2022.10067450.
[228] D. Cousineau, Fitting the three-parameter Weibull distribution: review and evaluation of existing and new methods, IEEE Trans. Dielectr. Electr. Insul. 16 (1) (2009) 281–288, https://doi.org/10.1109/TDEI.2009.4784578.
[229] H.K.T. Ng, L. Luo, Y. Hu, F. Duan, Parameter estimation of three-parameter Weibull distribution based on progressively type-II censored samples, J. Stat. Comput. Simulat. 82 (11) (2012) 1661–1678, https://doi.org/10.1080/00949655.2011.591797.
[230] K.E. Ahmad, Modified weighted least-squares estimators for the three-parameter Weibull distribution, Appl. Math. Lett. 7 (5) (1994) 53–56, https://doi.org/10.1016/0893-9659(94)90072-8.
[231] D. Jukić, M. Benšić, R. Scitovski, On the existence of the nonlinear weighted least squares estimate for a three-parameter Weibull distribution, Comput. Stat. Data Anal. 52 (9) (2008) 4502–4511, https://doi.org/10.1016/j.csda.2008.03.001.
[232] D. Marković, D. Jukić, M. Benšić, Nonlinear weighted least squares estimation of a three-parameter Weibull density with a nonparametric start, J. Comput. Appl. Math. 228 (1) (2009) 304–312, https://doi.org/10.1016/j.cam.2008.09.025.
[233] H. Nagatsuka, A study of estimation for the three-parameter Weibull distribution based on doubly Type-II censored data using a least squares method, in: 2008 Second International Conference on Secure System Integration and Reliability Improvement, IEEE, 2008, July, pp. 158–165, https://doi.org/10.1109/SSIRI.2008.45.
[234] D. Cousineau, Nearly unbiased estimators for the three-parameter Weibull distribution with greater efficiency than the iterative likelihood method, Br. J. Math. Stat. Psychol. 62 (1) (2009) 167–191, https://doi.org/10.1348/000711007X270843.
[235] J. Madhumitha, G. Vijayalakshmi, Bayesian reliability estimates of linear/circular consecutive k-out-of-n: F system based on Weibull distribution, AIP Conf. Proc. 2516 (1) (2022, November), https://doi.org/10.1063/5.0108545. AIP Publishing.
[236] D. Kececioglu, Reliability Engineering Handbook, vol. 1, DEStech Publications, Inc, 2002.
[237] M.B. Sarıgül, *Mechanical Reliability Analysis Using Stress-Strength Interference Model and Engineering Application of Reliability: System Safety Assessment* (Master's Thesis, Middle East Technical University, 2019. http://etd.lib.metu.edu.tr/upload/12624628/index.pdf.
[238] M.L. Tiku, A.D. Akkaya, Robust Estimation and Hypothesis Testing, New Age International, 2004.
[239] P. McCullagh, Likelihood, in: Ten Projects in Applied Statistics, Springer International Publishing, Cham, 2023, pp. 327–347, https://doi.org/10.1007/978-3-031-14275-8_17.
[240] J.P. Baudry, M. Broniatowski, C. Thommeret, Aggregated tests based on supremal divergence estimators for non-regular statistical models, in: International Conference on Geometric Science of Information, Springer Nature Switzerland, Cham, 2023, August, pp. 136–144, https://doi.org/10.1007/978-3-031-38271-0_14.
[241] A. Shafiq, A.B. Çolak, T.N. Sindhu, Reliability investigation of exponentiated Weibull distribution using IPL through numerical and artificial neural network modelling, Qual. Reliab. Eng. Int. 38 (7) (2022) 3616–3631, https://doi.org/10.1002/qre.3155.
[242] T.N. Sindhu, A. Atangana, Reliability analysis incorporating exponentiated inverse Weibull distribution and inverse power law, Qual. Reliab. Eng. Int. 37 (6) (2021) 2399–2422, https://doi.org/10.1002/qre.2864.
[243] K. Nyuytiymbiy, Parameters and hyperparameters in machine learning and deep learning, Towards Data Science, 2020. https://towardsdatascience.com/paramete rs-and-hyperparameters-aa609601a9ac. Retrieved from.
[244] L. Hertel, J. Collado, P. Sadowski, J. Ott, P. Baldi, Sherpa: robust hyperparameter optimization for machine learning, SoftwareX 12 (2020) 100591, https://doi.org/10.1016/j.softx.2020.100591.
[245] J. Rijsdijk, L. Wu, G. Perin, S. Picek, Reinforcement learning for hyperparameter tuning in deep learning-based side-channel analysis, IACR Transactions on Cryptographic Hardware and Embedded Systems (2021) 677–707, https://doi.org/10.46586/tches.v2021.i3.677-707.
[246] L. Yang, A. Shami, On hyperparameter optimization of machine learning algorithms: theory and practice, Neurocomputing 415 (2020) 295–316, https://doi.org/10.1016/j.neucom.2020.07.061.
[247] P. Probst, A.L. Boulesteix, B. Bischl, Tunability: importance of hyperparameters of machine learning algorithms, J. Mach. Learn. Res. 20 (1) (2019) 1934–1965.
[248] J.J. Ye, X. Yuan, S. Zeng, J. Zhang, Difference of convex algorithms for bilevel programs with applications in hyperparameter selection, Math. Program. 198 (2) (2023) 1583–1616, https://doi.org/10.1007/s10107-022-01888-3.
[249] P. Schratz, J. Muenchow, E. Iturritxa, J. Richter, A. Brenning, Hyperparameter tuning and performance assessment of statistical and machine-learning algorithms using spatial data, Ecol. Model. 406 (2019) 109–120, https://doi.org/10.1016/j.ecolmodel.2019.06.002.
[250] P. Probst, M.N. Wright, A.L. Boulesteix, Hyperparameters and tuning strategies for random forest, Wiley Interdisciplinary Reviews: Data Min. Knowl. Discov. 9 (3) (2019) e1301, https://doi.org/10.1007/978-3-030-78191-0_1.
[251] B. Bischl, M. Binder, M. Lang, T. Pielok, J. Richter, S. Coors, M. Lindauer, Hyperparameter optimization: foundations, algorithms, best practices, and open challenges, Wiley Interdisciplinary Reviews: Data Min. Knowl. Discov. 13 (2) (2023) e1484, https://doi.org/10.1002/widm.1484.
[252] M. Jie, X. Xiao-Li, Z. Dong-Hua, Survey of fault prediction methods for rotating machineries, Process Automatica Instrumentation 32 (8) (2011) 1–3.
[253] K.S. Chen, T.C. Chang, Fuzzy testing model for the lifetime performance of products under consideration with exponential distribution, Ann. Oper. Res. 312 (1) (2022) 87–98, https://doi.org/10.1007/s10479-020-03578-9.

[254] G.C. Stone, R.G. Van Heeswijk, Parameter estimation for the Weibull distribution, IEEE Trans. Electr. Insul. (4) (1977) 253–261, https://doi.org/10.1109/TEI.1977.297976.
[255] W. Liu, Q. Wang, Y. Zhu, H. Chen, GRU: optimization of NPI performance, J. Supercomput. 76 (2020) 3542–3554, https://doi.org/10.1007/s11227-018-2634-9.
[256] R. Wan, S. Mei, J. Wang, M. Liu, F. Yang, Multivariate temporal convolutional network: a deep neural networks approach for multivariate time series forecasting, Electronics 8 (8) (2019) 876, https://doi.org/10.3390/electronics8080876.
[257] H. Xiaoyan, L. Bingjie, S. Jing, L. Hua, L. Guojing, A novel forecasting method for short-term load based on the TCN-GRU model, in: 2021 IEEE International Conference on Energy Internet (ICEI), IEEE, 2021, September, pp. 79–83, https://doi.org/10.1109/ICEI52466.2021.00020.
[258] J. Yan, L. Mu, L. Wang, R. Ranjan, A.Y. Zomaya, Temporal convolutional networks for the advance prediction of ENSO, Sci. Rep. 10 (1) (2020) 8055, https://doi.org/10.1038/s41598-020-65070-5.
[259] B. Zhang, Y. Qiu, Lane detection algorithm based on dilated convolution network, in: Proceedings of the 2021 4th International Conference on Artificial Intelligence and Pattern Recognition, 2021, September, pp. 212–217, https://doi.org/10.1145/3488933.3489025.
[260] J. Campbell, Castings, Elsevier, 2003.
[261] D.A. Snelling, C.B. Williams, A.P. Druschitz, Mechanical and material properties of castings produced via 3D printed moulds, Addit. Manuf. 27 (2019) 199–207, https://doi.org/10.1016/j.addma.2019.03.004.
[262] C.B. Carter, M.G. Norton, Ceramic Materials: Science and Engineering, vol. 716, Springer, New York, 2007, p. 712.
[263] K. Kumar, M.J. Kim, Y.J. Park, H.N. Kim, H.J. Ma, J.W. Lee, J.W. Ko, A twofold increase in Weibull modulus of hot-pressed Si3N4 ceramic by modified pressing profile, Mater. Today Commun. 32 (2022) 103979, https://doi.org/10.1016/j.mtcomm.2022.103979.
[264] D. Wong, M. Anwar, S. Debnath, A. Hamid, I. Sudin, The influence of matrix density on the Weibull modulus of natural fiber reinforced nanocomposites, in: Materials Science Forum, vol. 1074, Trans Tech Publications Ltd, 2022, December, pp. 3–9, https://doi.org/10.4028/p-c626c1.
[265] T.L. Wang, M.A. Khan, C.S. Feng, M.Z. Lin, G. Yasin, W.B. Liao, Parallel preparation of multi-component alloys with composition gradient distribution and their nonlinear microstructures and mechanical properties, J. Alloys Compd. 921 (2022) 166159, https://doi.org/10.1016/j.jallcom.2022.166159.
[266] W.S. Lei, Z. Yu, P. Zhang, G. Qian, Standardized Weibull statistics of ceramic strength, Ceram. Int. 47 (4) (2021) 4972–4993.
[267] S. Nohut, Three-parameter (3P) Weibull distribution for characterization of the strength of ceramics showing R-Curve behaviour, Ceram. Int. 47 (2) (2021) 2270–2279.
[268] J. He, L. Liu, H. Yang, M.R.M. Aliha, Using two and three-parameter Weibull statistical model for predicting the loading rate effect on low-temperature fracture toughness of asphalt concrete with the ENDB specimen, Theor. Appl. Fract. Mech. 121 (2022) 103471, https://doi.org/10.1016/j.tafmec.2022.103471.
[269] B. Yang, S. Qin, L. Xue, H. Chen, The reasonable range limit of the shape parameter in the Weibull distribution for describing the brittle failure behaviour of rocks, Rock Mech. Rock Eng. 54 (2021) 3359–3367, https://doi.org/10.1007/s00603-021-02414-1.
[270] C. Prakash, G. Singh, S. Singh, W.L. Linda, H.Y. Zheng, S. Ramakrishna, R. Narayan, Mechanical reliability and in vitro bioactivity of 3D-printed porous polylactic acid-hydroxyapatite scaffold, J. Mater. Eng. Perform. 30 (2021) 4946–4956, https://doi.org/10.1007/s11665-021-05566-x.
[271] M.E. Ghitany, B. Atieh, S. Nadarajah, Lindley distribution and its application, Math. Comput. Simulat. 78 (4) (2008) 493–506, https://doi.org/10.1016/j.matcom.2007.06.007.
[272] W.S. Lei, P. Zhang, Z. Yu, G. Qian, Statistics of ceramic strength: use ordinary Weibull distribution function or Weibull statistical fracture theory, Ceram. Int. 46 (13) (2020) 20751–20768.
[273] A. Garrido, R. Caro-Carretero, J.R. Jimenez-Octavio, A. Carnicero, M. Such, A new approach to fitting the three-parameter Weibull distribution: an application to glass ceramics, Commun. Stat. Theor. Methods 50 (14) (2021) 3403–3420.
[274] Y.Y. Zhao, E. Ma, J. Xu, Reliability of compressive fracture strength of Mg–Zn–Ca bulk metallic glasses: flaw sensitivity and Weibull statistics, Scripta Mater. 58 (6) (2008) 496–499.
[275] B. Zberg, E.R. Arata, P.J. Uggowitzer, J.F. Löffler, Tensile properties of glassy MgZnCa wires and reliability analysis using Weibull statistics, Acta Mater. 57 (11) (2009) 3223–3231.
[276] W.H. Zhou, F.H. Duan, Y.H. Meng, C.C. Zheng, H.M. Chen, A.G. Huang, Y. Li, Effect of alloying oxygen on the microstructure and mechanical properties of Zr-based bulk metallic glass, Acta Mater. 220 (2021) 117345.
[277] M.A. Meyers, K.K. Chawla, Mechanical Behavior of Materials, Cambridge University Press, 2008.
[278] Y.Y. Zhao, E. Ma, J. Xu, Reliability of compressive fracture strength of Mg–Zn–Ca bulk metallic glasses: flaw sensitivity and Weibull statistics, Scripta Mater. 58 (6) (2008) 496–499.
[279] J. Tinschert, D. Zwez, R. Marx, K.J. Anusavice, Structural reliability of alumina-, feldspar-, leucite-, mica-and zirconia-based ceramics, J. Dent. 28 (7) (2000) 529–535, https://doi.org/10.1016/S0300-5712(00)00030-0.
[280] M. Roos, C. Schatz, B. Stawarczyk, Two independent prospectively planned blinded Weibull statistical analyses of flexural strength data of zirconia materials, Materials 9 (7) (2016) 512, https://doi.org/10.3390/ma9070512.
[281] E. Beyabanaki, R.E. Ashtiani, M. Moradi, M. Namdari, D. Mostafavi, A. Zandinejad, Biaxial flexural strength and Weibull characteristics of a resin ceramic material after thermal cycling, J. Prosthodont. 32 (8) (2023) 721–727, https://doi.org/10.1111/jopr.13622.
[282] R. Danzer, T. Lube, P. Supancic, R. Damani, Fracture of ceramics, Adv. Eng. Mater. 10 (4) (2008) 275–298, https://doi.org/10.1002/adem.200700347.
[283] J.B. Quinn, G.D. Quinn, A practical and systematic review of Weibull statistics for reporting strengths of dental materials, Dent. Mater. 26 (2) (2010) 135–147, https://doi.org/10.1016/j.dental.2009.09.006.
[284] H. Rinne, The Weibull Distribution: a Handbook, CRC press, 2008.
[285] S. Nohut, Influence of sample size on strength distribution of advanced ceramics, Ceram. Int. 40 (3) (2014) 4285–4295, https://doi.org/10.1016/j.ceramint.2013.08.093.
[286] M. Roos, B. Stawarczyk, Evaluation of bond strength of resin cement using different general-purpose statistical software packages for two-parameter Weibull statistics, Dent. Mater. 28 (7) (2012) e76–e88, https://doi.org/10.1016/j.dental.2012.04.013.
[287] L. Bütikofer, B. Stawarczyk, M. Roos, Two regression methods for estimation of a two-parameter Weibull distribution for reliability of dental materials, Dent. Mater. 31 (2) (2015) e33–e50, https://doi.org/10.1016/j.dental.2014.11.014.
[288] S. Greenland, Bayesian perspectives for epidemiological research: I. Foundations and basic methods, Int. J. Epidemiol. 35 (3) (2006) 765–775, https://doi.org/10.1093/ije/dyi312.
[289] L. Raubenheimer, Discussion of "Specifying prior distributions in reliability applications", Appl. Stoch Model Bus. Ind. (2023) https://doi.org/10.1002/asmb.2806.
[290] S.M. AbouRizk, D.W. Halpin, Statistical properties of construction duration data, J. Construct. Eng. Manag. 118 (3) (1992) 525–544, https://doi.org/10.1061/(ASCE)0733-9364(1992)118:3(525.
[291] K.M. Nassar, H.G. Gunnarsson, M.Y. Hegab, Using Weibull analysis for evaluation of cost and schedule performance, J. Construct. Eng. Manag. 131 (12) (2005) 1257–1262, https://doi.org/10.1061/(ASCE)0733-9364(2005)131:12(1257.
[292] A. Khalili, K. Kromp, Statistical properties of Weibull estimators, J. Mater. Sci. 26 (1991) 6741–6752, https://doi.org/10.1007/BF00553701.
[293] J.B. Wachtman, W.R. Cannon, M.J. Matthewson, Mechanical Properties of Ceramics, John Wiley & Sons, 2009.
[294] J.A. Salem, M.G. Jenkins, Standardization efforts for mechanical testing and design of advanced ceramic materials and components, in: 5th Conference on Aerospace Materials, Processes, and Environmental Technology, 2003, November.
[295] L. Wang, R. Dou, G. Wang, Y. Li, M. Bai, D. Hall, Y. Chen, Fracture strength and Weibull analysis of Ba0. 5Sr0. 5Co0. 8Fe0. 2O3− δ oxygen transport membranes evaluated by biaxial and uniaxial bending tests, Materials Science and Engineering: A 670 (2016) 292–299, https://doi.org/10.1016/j.msea.2016.06.029.

[296] J.A. Meganck, M.J. Baumann, E.D. Case, L.R. McCabe, J.N. Allar, Biaxial flexure testing of calcium phosphate bioceramics for use in tissue engineering, J. Biomed. Mater. Res. Part A: An Official Journal of The Society for Biomaterials, The Japanese Society for Biomaterials, and The Australian Society for Biomaterials and the Korean Society for Biomaterials 72 (1) (2005) 115–126, https://doi.org/10.1002/jbm.a.30213.
[297] A.Q. Morrison, Elastic Modulus and Biaxial Fracture Strength of Thermally Fatigued Hot-Pressed LAST and LASTT Thermoelectric Materials, Michigan State University, 2010.
[298] N. Shrestha, Factor analysis as a tool for survey analysis, Am. J. Appl. Math. Stat. 9 (1) (2021) 4–11.
[299] [online]. Available: www.riansclub.com/factor-of-safety/.
[300] F.B. Abifarin, Z. Musa, J.K. Abifarin, Mechanical processing of hydroxyapatite through sintering and multi-objective optimization technique for biomedical application, MRS Advances (2023) 1–6, https://doi.org/10.1557/s43580-023-00517-1.
[301] A.J. Wang, D.L. McDowell, Yield surfaces of various periodic metal honeycombs at intermediate relative density, Int. J. Plast. 21 (2) (2005) 285–320, https://doi.org/10.1016/j.ijplas.2003.12.002.
[302] K.G. Ewsuk, D.T. Ellerby, C.B. DiAntonio, Analysis of nanocrystalline and microcrystalline ZnO sintering using master sintering curves, J. Am. Ceram. Soc. 89 (6) (2006) 2003–2009, https://doi.org/10.1111/j.1551-2916.2006.00990.x.
[303] R. Deluzarche, B. Cambou, J.J. Fry, Modelling of rockfill behaviour with crushable particles, in: Numerical Modeling in Micromechanics via Particle Methods, Routledge, 2017, pp. 219–224.
[304] C. Salot, P. Gotteland, P. Villard, Influence of relative density on granular materials behaviour: DEM simulations of triaxial tests, Granul. Matter 11 (4) (2009) 221–236, https://doi.org/10.1007/s10035-009-0138-2.
[305] L. Gorjan, M. Ambrožič, Bend strength of alumina ceramics: a comparison of Weibull statistics with other statistics based on a very large experimental data set, J. Eur. Ceram. Soc. 32 (6) (2012) 1221–1227, https://doi.org/10.1016/j.jeurceramsoc.2011.12.010.
[306] M.A. Alabdullah, N.M. Ghoniem, A probabilistic-phase field model for the fracture of brittle materials, Model. Simulat. Mater. Sci. Eng. (2023), https://doi.org/10.1088/1361-651X/ad09ea.
[307] N. Kumar, F. Ghani, M.A. Fareed, S. Riaz, Z. Khurshid, M.S. Zafar, Bi-axial flexural strength of resin based dental composites–Influence and reliability of the testing method configuration, Mater. Technol. 37 (12) (2022) 2166–2172, https://doi.org/10.1080/10667857.2021.1886664.
[308] S.J. Lorenz, F. Sadeghi, A. Sharma, C. Wang, B. Wang, An investigation into various failure criteria on rolling contact fatigue through an improved probabilistic model, Tribol. Int. 188 (2023) 108875, https://doi.org/10.1016/j.triboint.2023.108875.
[309] P. Kittl, G. Diaz, Weivull's fracture statistics, or probabilistic strength of materials: state of the art, Res. Mech. 24 (2) (1988) 99–207.
[310] R. Danzer, T. Lube, P. Supancic, Monte Carlo simulations of strength distributions of brittle materials–type of distribution, specimen and sample size, Int. J. Mater. Res. 92 (7) (2022) 773–783, https://doi.org/10.1515/ijmr-2001-0143.
[311] R. Danzer, A. Börger, P. Supancic, M.A. Ruiz Villanueva, Ein einfacher Festigkeitsversuch für Scheiben aus spröden Werkstoffen, Mater. Werkst. 34 (5) (2003) 490–498, https://doi.org/10.1002/mawe.200390098.
[312] A. Nevarez-Rascon, A. Aguilar-Elguezabal, E. Orrantia, M.H. Bocanegra-Bernal, Compressive strength, hardness and fracture toughness of Al2O3 whiskers reinforced ZTA and ATZ nanocomposites: Weibull analysis, Int. J. Refract. Metals Hard Mater. 29 (3) (2011) 333–340, https://doi.org/10.1016/j.ijrmhm.2010.12.008.
[313] P.R.D. Marinho, R.B. Silva, M. Bourguignon, G.M. Cordeiro, S. Nadarajah, AdequacyModel: an R package for probability distributions and general purpose optimization, PLoS One 14 (8) (2019) e0221487, https://doi.org/10.1371/journal.pone.0221487.
[314] T. Fett, E. Ernst, D. Munz, D. Badenheim, R. Oberacker, Weibull analysis of ceramics under high stress gradients, J. Eur. Ceram. Soc. 23 (12) (2003) 2031–2037, https://doi.org/10.1016/S0955-2219(03)00024-4.
[315] R. Zhao, C. Ma, H. He, D. Han, H. Wang, R. Zhang, G. Shao, Enhanced flexural strength of pre-densified ZrO2 ceramics by a facile method of flash treatment, J. Mater. Res. Technol. (2023), https://doi.org/10.1016/j.jmrt.2023.11.023.
[316] S. Rujitanapanich, P. Kumpapan, P. Wanjanoi, Synthesis of hydroxyapatite from oyster shell via precipitation, Energy Proc. 56 (2014) 112–117, https://doi.org/10.1016/j.egypro.2014.07.138.
[317] R.B. Abernethy, J.E. Breneman, C.H. Medlin, G.L. Reinman, Weibull Analysis Handbook, 1983.
[318] R. Arnold, Discussion of: specifying prior distributions in reliability applications, Appl. Stoch Model Bus. Ind. (2023), https://doi.org/10.1002/asmb.2791.
[319] N. Isaacson, K. Lopez-Ambrosio, L. Chubb, N. Waanders, E. Hoffmann, C. Witt, D.A. Prawel, Compressive properties and failure behavior of photocast hydroxyapatite gyroid scaffolds vary with porosity, J. Biomater. Appl. 37 (1) (2022) 55–76, https://doi.org/10.1177/08853282211073.
[320] N. Ilie, N.E. Serfoezoe, D. Prodan, J. Diegelmann, M. Moldovan, Synthesis and performance of experimental resin-based dental adhesives reinforced with functionalized graphene and hydroxyapatite fillers, Mater. Des. 221 (2022) 110985, https://doi.org/10.1016/j.matdes.2022.110985.
[321] A. Galotta, K. Rubenis, J. Locs, V.M. Sglavo, Dissolution-precipitation synthesis and cold sintering of mussel shells-derived hydroxyapatite and hydroxyapatite/chitosan composites for bone tissue engineering, Open Ceramics 15 (2023) 100418, https://doi.org/10.1016/j.oceram.2023.100418.
[322] L. D'Andrea, D. Gastaldi, F. Baino, E. Verné, G. Saccomano, L. D'Amico, P. Vena, Mechanical characterization of miniaturized 3D-printed hydroxyapatite parts obtained through vat photopolymerization: an experimental study, J. Mech. Behav. Biomed. Mater. 141 (2023) 105760, https://doi.org/10.1016/j.jmbbm.2023.105760.
[323] F. Baino, G. Magnaterra, E. Fiume, A. Schiavi, L.P. Tofan, M. Schwentenwein, E. Verné, Digital light processing stereolithography of hydroxyapatite scaffolds with bone-like architecture, permeability, and mechanical properties, J. Am. Ceram. Soc. 105 (3) (2022) 1648–1657, https://doi.org/10.1111/jace.17843.
[324] D. Marovic, M. Par, K. Posavec, I. Marić, D. Štajdohar, A. Muradbegović, Z. Tarle, Long-term assessment of contemporary ion-releasing restorative dental materials, Materials 15 (12) (2022) 4042, https://doi.org/10.3390/ma15124042.
[325] X. Zhao, P. Wang, J. Zheng, J. Liu, Z. Yang, L. Yang, Preparation of multilayered C–Si–Al2O3 coatings on continuous carbon fibers and C–Si–Al2O3-coated carbon-fiber-reinforced hydroxyapatite composites, Ceram. Int. 48 (18) (2022) 26028–26041, https://doi.org/10.1016/j.ceramint.2022.05.285.
[326] J. Huang, S. E, L. Si, J. Li, Z. Tian, Z. Lu, Composite films of hydroxyethyl cellulose and hydroxyapatite nanowires with high mechanical strength and electrical insulation property, J. Wood Chem. Technol. 42 (1) (2022) 15–25, https://doi.org/10.1080/02773813.2021.1998128.
[327] A. Karimi, M.H. Paydar, Investigation on the mechanical behavior and fracture mode of ice-templated NiO-ysz anode electrode for solid oxide fuel cells application, J. Mater. Eng. Perform. (2023) 1–8, https://doi.org/10.1007/s11665-023-08419-x.
[328] C. Tuncer, M. Güden, M. Orhan, M.K. Sarıkaya, A. Taşdemirci, Quasi-static and dynamic Brazilian testing and failure analysis of a deer antler in the transverse to the osteon growth direction, J. Mech. Behav. Biomed. Mater. 138 (2023) 105648, https://doi.org/10.1016/j.jmbbm.2023.105648.
[329] K. Przystupa, Research on the durability and reliability of industrial layered coatings on metal substrate due to abrasive wear, Materials 16 (5) (2023) 1779, https://doi.org/10.3390/ma16051779.
[330] M. Par, L. Plančak, L. Ratkovski, T.T. Tauböck, D. Marovic, T. Attin, Z. Tarle, Improved flexural properties of experimental resin composites functionalized with a customized low-sodium bioactive glass, Polymers 14 (20) (2022) 4289, https://doi.org/10.3390/polym14204289.
[331] R.S. Monteiro, B.M. Ferrairo, L.J. de Azevedo-Silva, P.R. Minim, J.H. Rubo, A.Y. Furuse, A.F.S. Borges, Glass ceramics behave like selectively etched enamel on interfaces produced with self-adhesive/self-curing resin cement, Int. J. Adhesion Adhes. 124 (2023) 103383, https://doi.org/10.1016/j.ijadhadh.2023.103383.

[332] E.J. Lira dos Santos, F. Campos, A.M.X. Dantas, M.L.L.A. Lira, V.F. Wandsher, N.R.D. Silva, R.O.D.A. Souza, Bond strength and Weibull analysis of fiber posts luted with different cement types and mechanically aged, J. Adhes. Sci. Technol. 36 (7) (2022) 762–773, https://doi.org/10.1080/01694243.2021.1938473.
[333] Faria, D., Sahoo, N., Monteiro, F., Garrett, G., Silva, F., & Carvalho, O. Direct Laser Writing (Dlw)-Based Biofunctionalization of Ti6al4v for Enhanced Osseointegration of Implants. Available at *SSRN 4562312*. SSRN: https://ssrn.com/abstract=4562312orhttps://doi.org/10.2139/ssrn.4562312.
[334] N. Ilie, Comparison of modern light-curing hybrid resin-based composites to the tooth structure: static and dynamic mechanical parameters, J. Biomed. Mater. Res. B Appl. Biomater. 110 (9) (2022) 2121–2132, https://doi.org/10.1002/jbm.b.35066.
[335] W. Liao, J. Hu, Y. Zhang, Micro forming and deformation behaviors of Zr50. 5Cu27. 45Ni13. 05Al9 amorphous wires, Intermetallics 20 (1) (2012) 82–86, https://doi.org/10.1016/j.intermet.2011.08.021.
[336] R. Liu, X. Wang, J. Liu, Y. Zhang, G. Cao, Z. Liu, M. Zhang, Correlation of microstructural evolution and tensile mechanical behavior of Gd–Al–Co–Fe series "metallic glass" fibers, J. Mater. Res. Technol. 14 (2021) 1390–1400, https://doi.org/10.1016/j.jmrt.2021.07.053.
[337] S. Wang, F. Guo, Z. Ning, H. Bai, H. Li, H. Fan, Y. Huang, The effect of cold drawing on the structure, tensile fracture strength and reliability of CuZrAl amorphous microwires, Materials Science and Engineering: A 881 (2023) 145421, https://doi.org/10.1016/j.msea.2023.145421.
[338] O.A. Osuchukwu, A. Salihi, I. Abdullahi, D.O. Obada, Synthesis and characterization of sol–gel derived hydroxyapatite from a novel mix of two natural biowastes and their potentials for biomedical applications, Mater. Today: Proc. 62 (2022) 4182–4187, https://doi.org/10.1016/j.matpr.2022.04.696.
[339] O.A. Osuchukwu, A. Salihi, I. Abdullahi, B. Abdulkareem, K.A. Salami, P.O. Etinosa, D.O. Obada, Pedagogical approach for the development and optimization of a novel mix of biowastes-derived hydroxyapatite using Box-Behnken experimental design, Heliyon (2023) 145421, https://doi.org/10.1016/j.heliyon.2023.e23092.
[340] S. Warangkulkasemkit, P. Pumpaluk, Comparison of physical properties of three commercial composite core build-up materials, Dent. Mater. J. 38 (2) (2019) 177–181, https://doi.org/10.4012/dmj.2018-038.